Chapter 3

Sequence Specific Detection of DNA Using Self-Quenched Fluorophore-Polyamide Conjugates

The text of Chapter 3A was taken in part from a manuscript coauthored with Victor Rucker, Christian Melander, and Professor Peter Dervan (California Institute of Technology).

Rucker, V. C.; Foister, S.; Melander, C. M.; Dervan, P. B. "Sequence Specific Fluorescent Detection of Double Strand DNA" *J. Am. Chem. Soc.* **2003**, *125*, 1195-1202.

Chapter 3B describes ongoing research. Work towards chromosome staining done in collaboration with Ben Edelson, Tim Best (Dervan Group; Caltech) and Edward Ramos (Trask Group; University of Washington).

Work on recognition of purine repeat sequences done in collaboration with Adam Urbach (Dervan Group; Caltech).

Work in the field of single molecule recognition of DNA done in collaboration with Mark Unger and Ido Braslavsky (Quake Group; Caltech).

Abstract

Fluorescent methods for the sequence specific detection of DNA are vital to unraveling the functional, three-dimensional significance of the linear human genome. The ability of minor groove-binding polyamides to specifically target predetermined DNA sequences, without sample denaturation, in biologically relevant condensed states and protein complexes, offers appreciable advantages relative to existing PNA- or oligonucleotide-based DNA sensors. Chapter 3 describes the development of fluorophore-polyamide conjugates that exhibit pronounced fluorescent enhancement upon binding their cognate DNA sequences.

Chapter 3A discusses the synthesis and physical characterization of TMR-hairpin polyamide conjugates. The fluorescent properties of these compounds in the absence of DNA and in the presence of both match and mismatch DNA duplexes were evaluated. The sequence specificity of fluorescent enhancement was validated by correlation with observed association constants determined by quantitative DNase I footprinting. The use of TMR-hairpin conjugates to recognize non-Watson-Crick base pairs was also demonstrated.

Chapter 3B suggests applications of fluorophore-polyamide conjugates in genomic analysis. Centromere staining in the context of cytogenetic chromosome spreads, as well as in live cells, is discussed and the detection of other repeat sequences is proposed. Preliminary experiments addressing the suitability of polyamides in physical methods of DNA mapping are summarized.

Chapter 3A

Sequence Specific Fluorescence Detection of Double Strand DNA

Background and Significance

Interest in the detection of specific nucleic acid sequences in homogeneous solution has increased due to major developments in human genetics. Single nucleotide polymorphisms (SNPs) are the most common form of variation in the human genome and can be diagnostic of particular genetic predispositions toward disease.[1] Most methods of DNA detection involve hybridization by an oligonucleotide probe to its complementary single-strand nucleic acid target leading to signal generation.[2-7] One example is the "molecular beacon" which consists of a hairpin DNA labeled in the stem with a fluorophore and a quencher.[4] Binding to a complementary strand results in opening of the hairpin and separation of the quencher and the fluorophore. However, detection by hybridization requires DNA *denaturation* conditions, and it remains a challenge to develop sequence specific fluorescent probes for DNA in the double strand form.[8-10]

Hairpin polyamides are a class of synthetic ligands that can be programmed to recognize specific DNA sequences with affinities and specificities comparable to DNA binding proteins.[11] The large number of DNA sequences which can be targeted with hairpin polyamides suggests that polyamide-fluorophore conjugates might be useful in fluorescence-based detection of specific nucleic acid sequences. Within the context of targeting sites in gigabase size DNA, Laemmli demonstrated

that polyamides with Texas Red or fluorescein at the C-terminus specifically stain 5'-GAGAA-3' repeats in *Drosophila* satellites, as well as teleomeric repeats in insect and human chromosomes (5'-TTAGG-3' and 5'-TTAGGG-3', respectively).[12] Similarly, Trask has demonstrated the use of polyamide-dye conjugates to fluorescently label specific repetitive regions on human chromosomes 9, Y and 1 (TTCCA repeats) for discrimination in cytogenetic preparations and flow cytometry.[13]

We report here that hairpin polyamide-fluorophore conjugates are capable of detecting specific sequences within short segments of double helical DNA in homogeneous solution (Figure 3.1). The fluorescence of our polyamide-tetramethyl rhodamine (TMR) conjugates is largely quenched in the absence of DNA. Addition of duplex DNA containing a match site to a polyamide-TMR conjugate affords a ≥10-fold increase in fluorescence. Attenuated signal results when mismatch DNA is added at the same concentration. This fluorescence detection method allows us to analyze the specificity of hairpin polyamides that target non-Watson-Crick base pairs.

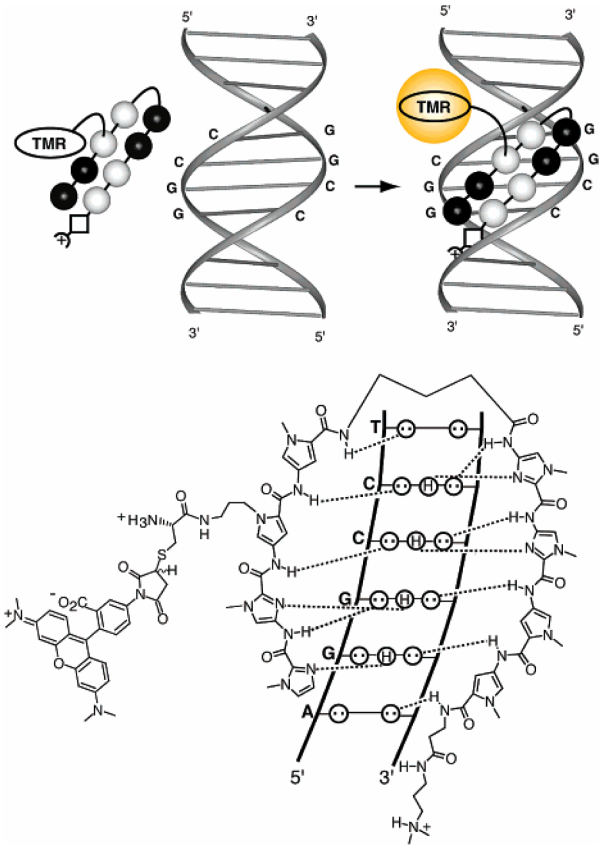

Figure 3.1 Binding models for self-quenched TMR-hairpin polyamide conjugates. These conjugates show pronounced fluorescent enhancement upon binding DNA (*top*) while recognizing DNA according to the described pairing rules (*bottom*).

Results and Discussion

Detection of Specific DNA Sequences in Homogeneous Solution. As a model study, six hairpin pyrrole-imidazole (Py-Im) polyamides with TMR[14] attached at an internal pyrrole ring were synthesized (Figure 3.2). Each eight-ring polyamide **1**-**6** was programmed according to the pairing rules[11] for a different 6-base pair DNA match sequence (Figure 3.3). Tetramethyl rhodamine-5-maleimide was coupled as a thioether to an internal pyrrole ring by a cysteine linker. This point of attachment was chosen to direct the fluorophore into aqueous solution (away from the DNA

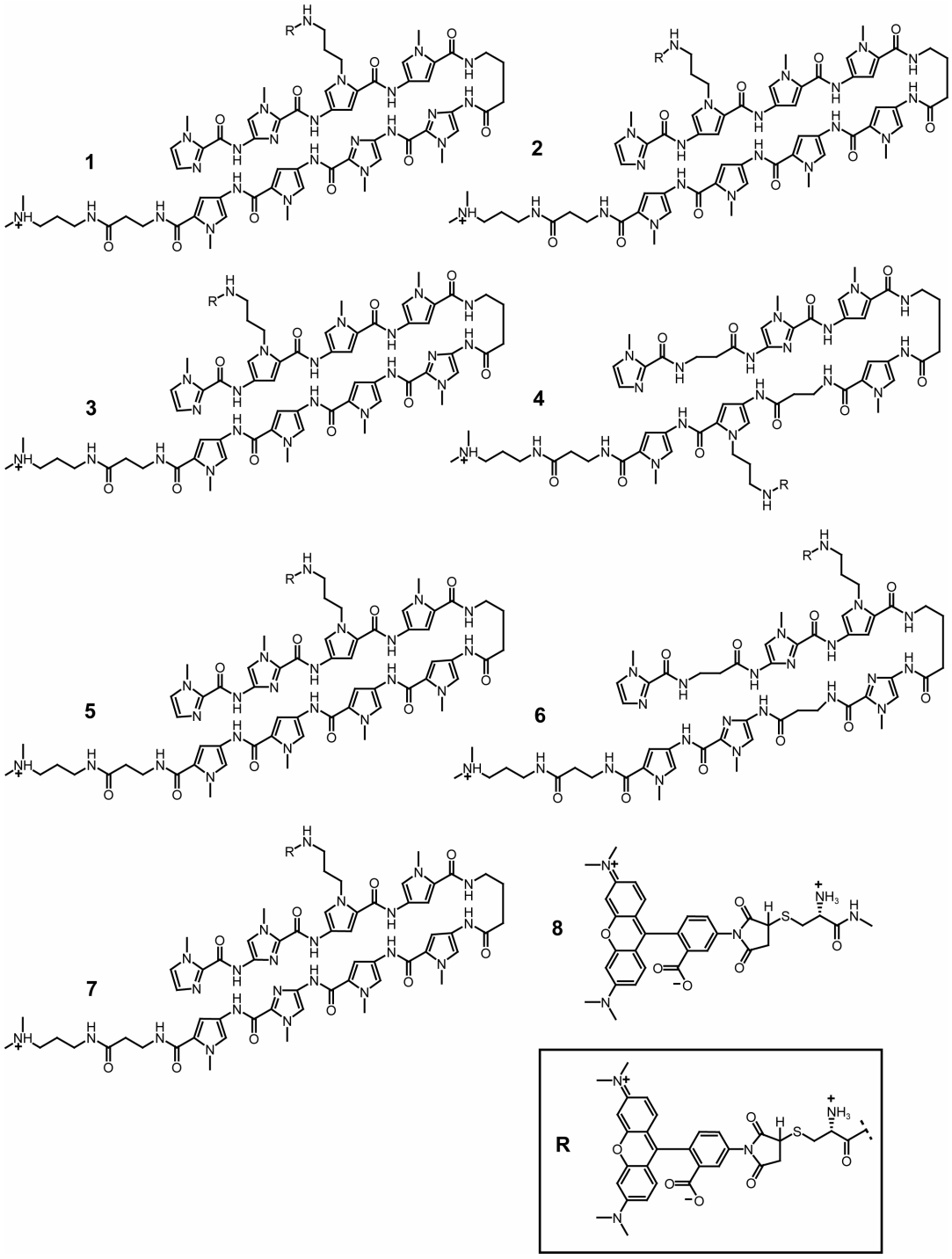

Figure 3.2 Chemical structures of TMR-hairpin polyamide conjugates and control compounds.

helix) to minimize possible unfavorable steric interactions when the hairpin is bound in the minor groove (Figure 3.1). The synthesis of fluorescent conjugates **1-7** is described in detail in Chapter 2.

The parent hairpins typically bind with equilibrium association constants K_a = 10^9 M^{-1}.[11] In order to determine the energetic consequences for covalent attachment of fluorophores at the N1 position of at internal pyrrole ring in the 8-ring hairpin, the equilibrium association constants for conjugates **1**-**6** at six sites were determined by quantitative footprinting titration. The affinities of conjugates **1**-**6** at DNA match sites are reduced by a factor of 10-50 from those of the parents (Table 3.1A).[11] Despite the energetic penalty, the expected sequence specificities are maintained: K_a (match) > K_a (single mismatch) > K_a (multiple mismatch) (Table 3.1B).

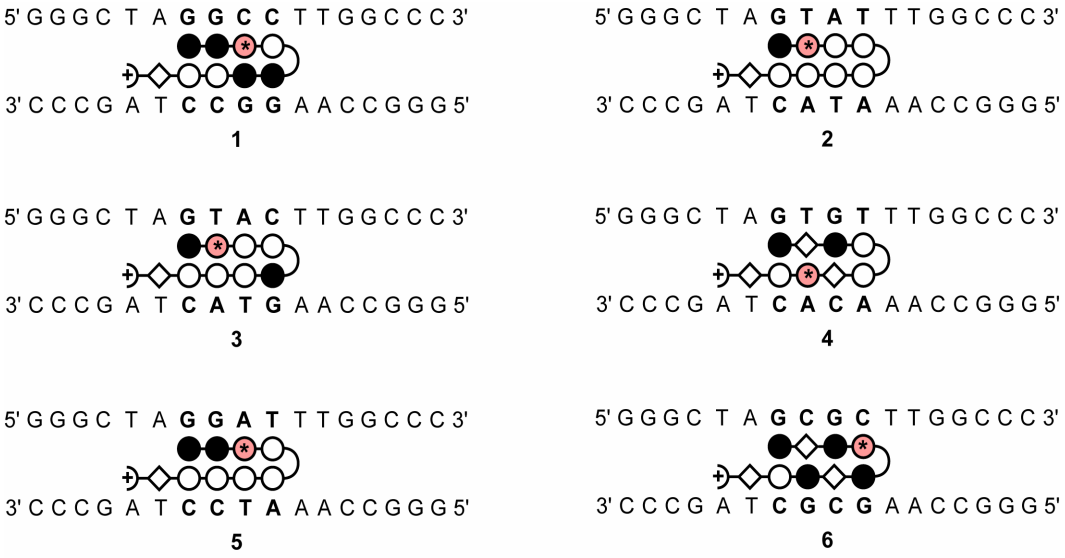

Figure 3.3 Ball-and-stick representations of hairpin conjugates bound to match duplex DNA sequences.

The fluorescence properties of the polyamide-TMR conjugates **1**-**6** in the presence and absence of short segments of duplex DNA (17-mer) were examined (Figure 3.4). The absorption maxima of conjugates **1**-**6** (~560 nm) are red-shifted and are attenuated relative to the absorption maximum (550 nm) of the TMR fluorophore **8** alone (Figure 3.4A), presumably due to electronic interactions

Table 3.1A Observed equilibrium association constants (M^{-1}) for 1-6.

Binding Site	1	2	3	4	5	6
5'-ta **GGCC** tt-3'	**2.1×10^9**	$< 10^7$	$< 10^7$	2.0×10^7	$\leq 2.8 \times 10^7$	$< 10^7$
5'-ta **GTAT** tt-3'	$< 10^7$	**2.5×10^8**	5.2×10^7	$\leq 5.2 \times 10^8$	$< 10^7$	$\leq 5.4 \times 10^7$
5'-ta **GTAC** tt-3'	$< 10^7$	5.0×10^7	**1.7×10^9**	$\leq 4.2 \times 10^8$	3.2×10^8	$\leq 1.4 \times 10^8$
5'-ta **GTGT** tt-3'	$< 10^7$	1.0×10^8	$< 10^7$	**1.4×10^9**	$\leq 4.5 \times 10^7$	$\leq 2.0 \times 10^8$
5'-ta **GGTA** tt-3'	$< 10^7$	1.0×10^8	$< 10^7$	1.1×10^8	**$\leq 9.7 \times 10^8$**	$< 10^7$
5'-ta **GCGC** tt-3'	$< 10^7$	$< 10^7$	$< 10^7$	3.0×10^7	$\leq 8.7 \times 10^7$	**$\leq 4.9 \times 10^8$**

Table 3.1B Normalized Association Constants for 1-6 (M^{-1}) for 1-6.

Binding Site	1	2	3	4	5	6
5'-ta **GGCC** tt-3'	**1**	< 0.05	< 0.01	0.01	≤ 0.03	≤ 0.02
5'-ta **GTAT** tt-3'	< 0.01	**1**	0.03	≤ 0.37	< 0.01	≤ 0.11
5'-ta **GTAC** tt-3'	< 0.01	0.20	**1**	≤ 0.30	0.33	≤ 0.29
5'-ta **GTGT** tt-3'	< 0.01	0.40	< 0.01	**1**	≤ 0.05	≤ 0.41
5'-ta **GGTA** tt-3'	< 0.01	0.40	< 0.01	0.08	**1**	< 0.02
5'-ta **GCGC** tt-3'	< 0.01	< 0.05	< 0.01	0.02	≤ 0.09	**1**

The assays were carried out at 22 °C at pH 7.0 in the presence of 10 mM Tris-HCl, 10 mM KCl, 10 mM $MgCl_2$, and 5 mM $CaCl_2$.

between the fluorophore and the polyamide in the ground state.[16] In the absence of DNA, the fluorescence intensities of the polyamide-TMR conjugates are significantly diminished relative to the TMR control **8** (pH 7.0, TKMC buffer). The addition of increasing amounts of match DNA to the conjugate affords an increase of fluorescence until a 1:1 DNA:conjugate stoichiometry is reached (Figure 3.4B-C). Using polyamide **3** as an example, fluorescence data from the addition of an increasing amount of a 17 base pair (17-mer) DNA duplex (0.05-1.0 μM concentration) containing the match sequence 5'-tAGTACTt-3' to an aqueous solution of 1 μM concentration of match conjugate **3** results in an increase in fluorescence intensity characteristic of all conjugates **1**-**6**. Fluorescent enhancement is greatest when the DNA duplex contains the polyamide's match sequence (Table

3.2). Addition of 17-bp DNA duplex containing a match sequence beyond the 1:1 DNA:polyamide stoichiometry does not lead to further significant increase of

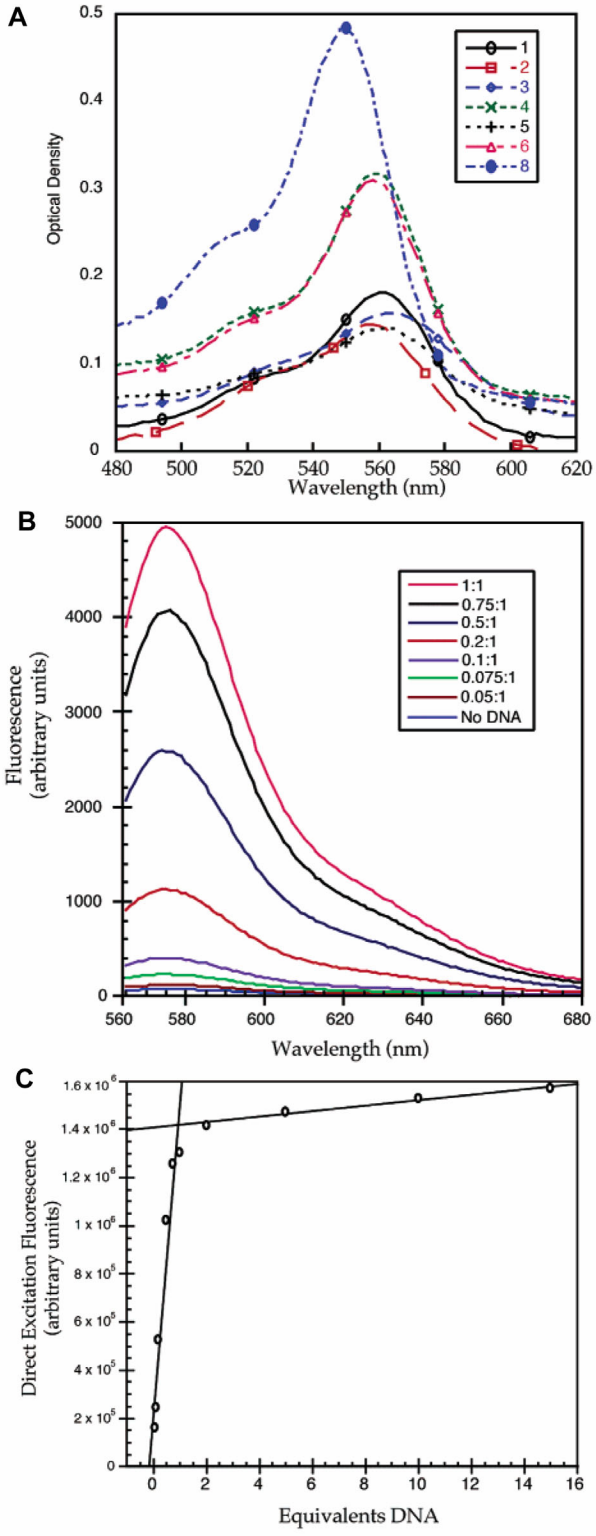

Figure 3.4 Spectroscopic properties of TMR-hairpin conjugates. **(A)** Absorption spectra of **1**-**6**, **8**. **(B)** Fluorescence emission profile for compound **3** (1 μM) in the presence of increasing concentrations of match duplex DNA (0.05-1 μM). **(C)** Direct excitation data for compound **3** with various concentrations of DNA.

Table 3.2 Normalized fluorescent intensities for 1-6 (1μM) with DNA duplexes (1μM).

Binding Site	1	2	3	4	5	6
5'-t a **G G C C** t t-3'	**1**	0.04	0.03	0.04	0.05	0.08
5'-t a **G T A T** t t-3'	0.04	**1**	0.09	0.30	0.20	0.10
5'-t a **G T A C** t t-3'	0.02	0.22	**1**	0.12	0.01	0.27
5'-t a **G T G T** t t-3'	0.04	0.30	0.01	**1**	0.08	0.18
5'-t a **G G T A** t t-3'	0.05	0.13	0.03	0.09	**1**	0.07
5'-t a **G C G C** t t-3'	0.07	0.02	0.05	0.07	0.04	**1**

The assays were carried out at 22 °C at pH 7.0 in the presence of 10 mM Tris-HCl, 10 mM KCl, 10 mM $MgCl_2$, and 5 mM $CaCl_2$.

emission intensity which indicates the occurrence of a single binding event between the conjugate and each DNA duplex (Figure 3.4C).

For the most effective discrimination, the stabilities of the different polyamide-DNA complexes should be match > single base mismatch > multiple base mismatch as determined from our footprinting study (Table 3.1). The ability of each conjugate **1**-**6** to distinguish one match from an ensemble of six different DNA sequences by fluorescence was examined by direct laser excitation scanning through the bottom of polystyrene plates. The data were acquired on a Molecular Dynamics Typhoon optical scanner employing a 532 nm 10-20 mW excitation laser and a 580 nm emission filter (±15 nm fwhm) suitable for TMR fluorescence detection. The emission data for hairpin polyamide conjugates **1**-**6** interacting with six different double stranded 17-mers is presented in Figure 3.5A. Polyamide-TMR conjugates are mostly quenched, except in the presence of increasing concentrations of a match DNA sequence. The data were normalized and plotted against the concentration of DNA titrant (0.02 μM to 1 μM) added to a 1 μM solution of conjugate (Figure 3.5B). The 1:1 stoichiometry end point provides a measure of the relative sequence specificity of each polyamide-TMR conjugate **1**-**6**. We note the agreement

between the normalized specificities determined by DNase I footprinting titration (Table 3.1B) and those we observe from this new optical assay (Table 3.2).

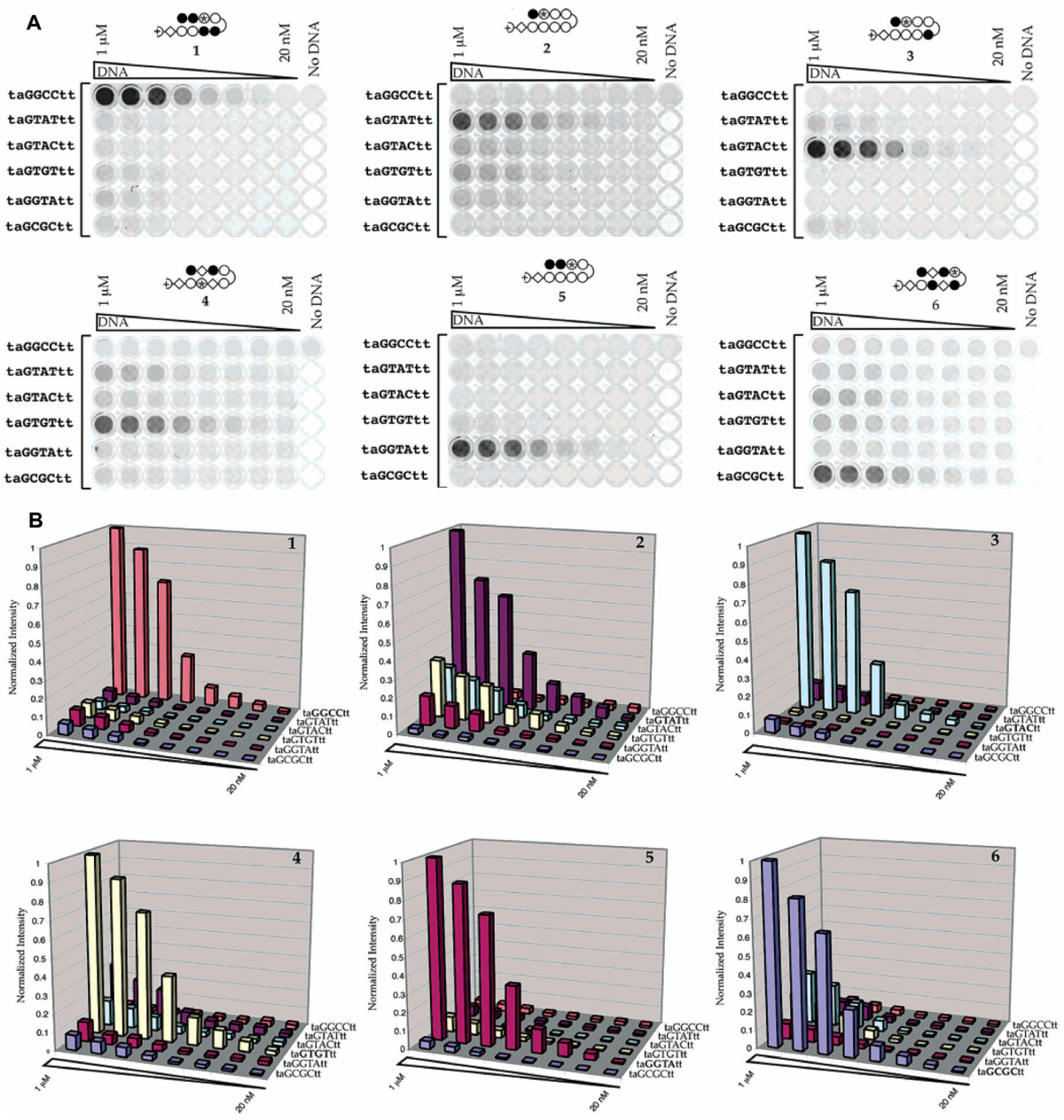

Figure 3.5 TMR-polyamide conjugate microplate experiments. **(A)** Conjugates **1**-**6** titrated with increasing concentrations (0.02-1 μM) of six different DNA duplexes. Data was collected using Typhoon imaging system with increasing fluorescent intensity (580 nm) correlated by darkness of wells. **(B)** Normalized observed fluorescent intensities from microplate experiments.

The observation that the fluorescence of the TMR fluorophore is significantly diminished when attached by a short tether to an internal pyrrole ring position in a series of hairpin polyamide-TMR conjugates was not expected. We have found that other fluorophores, such as fluorescein, when conjugated to an internal pyrrole of hairpin polyamides behave similarly. Presumably, the short linker holds the fluorophore in very close proximity or in direct contact with the hairpin polyamide. After excitation, the polyamide-fluorophore decays from the excited state via a nonradiative pathway. Incorporation of the aliphatic β-alanine (β) residues leads to a decrease in fluorescence quenching. The more flexible aliphatic β may allow increased conformational freedom to the conjugates **4** and **6**, possibly disrupting the association of dye and polyamide. The perturbed ground-state absorption spectrum of the fluorophore suggests a molecular association between polyamide and fluorophore that allows quenching to occur.[17]

The simplest model is that, upon binding DNA, the hairpin is sequestered in the minor groove moving the TMR fluorophore away from the polyamide and into the surrounding aqueous environment. One can imagine two conformations for the polyamide-dye conjugate: polyamide and TMR are in close proximity when free in solution (fluorescence quenched), and polyamide and TMR are separated in an extended conformation with the TMR projecting away from the polyamide when bound to DNA (fluorescence unquenched).

Both Laemmli and Trask have demonstrated the utility of polyamide-dye conjugates in the context of *gigabase size* DNA as sequence specific chromosome "paints".[12,13] This report extends the arsenal of applications for polyamide-dye molecules to specific DNA sequence detection in solution *within short segments* of DNA. The short segments of DNA are not immobilized on a chip nor is there a need for end labeling. It may be that applications might be related to "SNP typing" in which the identity of the SNP containing sequence is known. In a formal sense, recognition and detection in these bifunctional polyamide-dye molecules can be tuned separately; the polyamide module is programmed for a desired DNA sequence by the pairing rules and the dye is chosen for optimal absorption/emission properties.[18]

Polyamides as Molecular Calipers for Non-Watson-Crick Base Pairs in the DNA Minor Groove. Our fluorescence DNA detection method allows us to screen, in parallel, how a hairpin polyamide will behave when it is forced to bind over a non-Watson-Crick base pair. To date, the energetics of polyamide binding over non-Watson-Crick base pairs has not been examined, mainly due to the labor intensive effort required for the preparation of special end-radiolabeled DNA fragments containing discrete non-Watson-Crick base pairs for use in quantitative footprinting titration analysis. Three hairpin polyamide-fluorophore conjugates **3**, **5**, and **7** were used to screen Py/Py, Im/Py, and Im/Im ring pairs, respectively, against all possible 16 pairing permutations of the nucleic acid bases A, T, G, and C (Figure 3.6). Polyamide **7** contains an unusual Im/Im ring pairing, previously shown to be energetically unfavorable for recognition of any of the four Watson-Crick base

pairings.[19] However, Wang and co-workers have reported an NMR structure for the polyamide dimer $(ImImImDp)_2$ that indicates binding with a minor groove site containing G•T and T•G base pairs under the Im/Im pair.[20] Im/Im recognition of a G•T and T•G wobble mismatch is the first example of ring pairs for specific recognition of non-Watson-Crick base pairs.[21]

Hairpin-forming oligonucleotides (37-mer) were synthesized and annealed (pH 7.0, tris-EDTA buffer). Each duplex was designed to allow for base pair variance at a single unique X/Y position within the context of a 6-base pair hairpin match site. Assays were conducted in 30 μL solutions with the concentration of polyamide conjugate fixed at 1 μM, and the concentration of oligonucleotide was varied from 0.1 μM to 1 μM. After 4 h incubation (22 °C), fluorescence intensities at the 16 variable positions were acquired in parallel on the optical scanner (16 *X*/*Y* positions × 5 concentrations).

Figure 3.6 shows the data collected by direct excitation fluorescence and the normalized data represented in bar graph format. Polyamide **3** and **5** reveal strong fluorescence intensity, and hence affinity, for a sequence containing a match site as dictated by the pairing rules, i.e., Py/Py prefers A•T and T•A over the 14 other base pairs; Im/Py prefers G•C over the 15 other base pairs. Polyamide **8** with the Im/Im pair shows a slight preference for G/C over A/T, but does not discriminate G•C from C•G as expected for a symmetrical ring pair. Remarkably, the Im/Im pair binds T•G with the highest affinity validating the Lee-Sugiyama-Wang model.[20] However, in our study Im/Im distinguishes T•G from G•T, a result not anticipated in the NMR

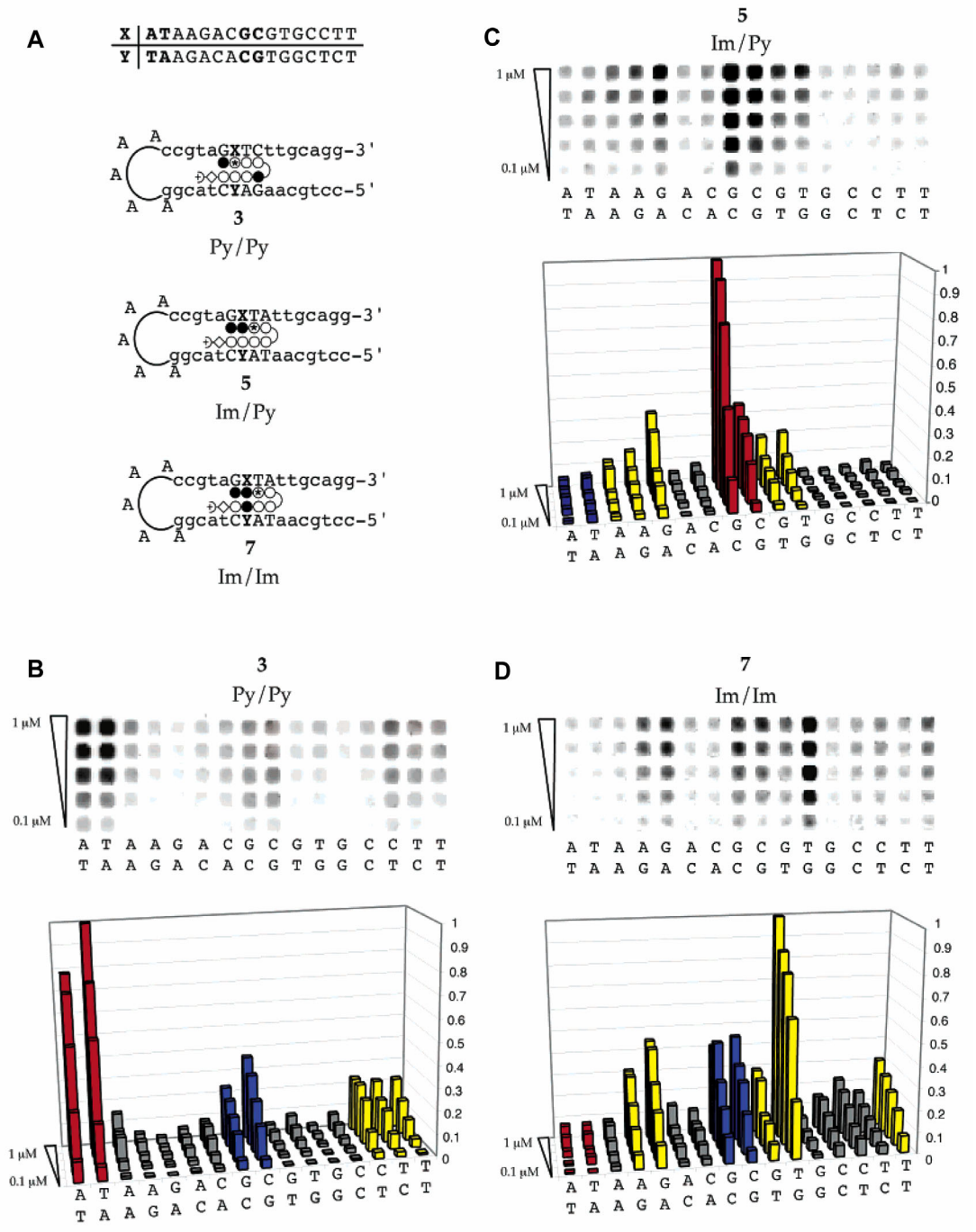

Figure 3.6 Non-Watson-Crick base pair recognition by TMR-polyamide conjugates. **(A)** Design of hairpin duplex oligonucleotides containing all 16 possible base pairs at a single X/Y position. **(B-D)** Fluorescent intensities obtained on Typhoon scanner for conjugates **3**, **5**, and **7** titrated against the 16 hairpin duplexes.

structure, which may be due to different sequence contexts used in the two

experiments. It is noteworthy that a minor groove binding polyamide can target *a single non-Watson-Crick base pair* out of 12 unique possibilities.

In summary, polyamide-fluorophore conjugates have been used to target sequence repeats in chromosomes for interrogation of sequence location and estimation of repeat length.[12,13] In this study, we extend the use of polyamide-fluorophore conjugates to distinguish match and mismatch sequences within short segments of DNA in solution. The correlation of sequence identity with fluorescence enhancement may be useful in other applications such as screening for sequence variation in specific segments of genomic DNA.

Experimental Section

Materials

Water was from either a Millipore MilliQ water purification system or RNase free water from a USB. All buffers were 0.2 μm filtered prior to storage. Oligonucleotides were synthesized and purified by The Caltech Biopolymer Synthesis and Analysis Resource Center and Genbase Inc., San Diego. Enzymes for molecular biology were purchased from either New England Biolabs or Boeringer-Mannheim. [α-^{32}P] adenosine triphosphate and [α-^{32}P] thymidine triphosphate were purchased from New England Nuclear. Polystyrene plates were from VWR Scientific. Fluorescence spectrophotometer measurements were made at room temperature on an ISS K2 spectrophotometer employing 5 nm emission and excitation slits in conjunction with a Hg lamp. Polystyrene plate measurements were made on a Molecular Dynamics Typhoon employing a 532 nm 10-20 mW excitation laser. The emission filter employed is 580 ± 15 nm filter for observation of tetramethyl rhodamine fluorescence.

Synthesis of Polyamide-Fluorophore Conjugates

Polyamides **1**-**7** were synthesized by solid-phase methods as described in Chapter 2 (compounds **38**, **40**-**45**).

Optical Characterization

All measurements were performed in TKMC buffer {10 mM Tris-HCl (pH 7.0), 10 mM KCl, 10 mM $MgCl_2$, and 5 mM $CaCl_2$}. The concentration of polyamide-TMR conjugate was 1 μM and the volume of solution used for each measurement was 150 μL. In the fluorimeter, polyamides **1**-**6** were excited at 545 nm and measured over the interval of 570 nm to 680 nm. Emission maxima are 575 nm for **1**-**8**. 1 μM solutions of each conjugate were irradiated in the presence and absence of 1 μM of the appropriate match DNA to generate the fluorescence enhancements reported in Supplemental Figure S4. Absorption spectra for **1**-**6** and **8** were recorded under the same conditions as emission with **1**-**6** at higher concentration.

96-Well Plate Characterization

In the dark, 150 μL solutions were made by titrating together a fixed concentration of 1 μM conjugate against 20 nM to 1 μM of each DNA 17-mer. The solutions were gently swirled for a few minutes and then allowed to sit for 4 h before measurements were made. No changes in fluorescence intensity were observed for longer equilibration times. Plates containing polyamides **1**-**7** were excited at 532 nm, and data were collected at 580 (±15 nm fwhm) nm. ImageQuant software (Molecular Dynamics) was used to analyze the fluorescence intensity of each titration experiment. From these data, histograms were constructed to assist in determining DNA sequence preference for each conjugate. The normalized data used in each histogram is polyamide specific assuming the background to be the lowest observable fluorescence intensity, which is subtracted in the denominator

from the highest observed fluorescence intensity, that of the match sequence at 1:1 conjugate:duplex as given by the relation $(F_{obs} - F_{min})/(F_{max} - F_{min})$.

References

1) a. Wang, D. G.; Fan, J.-B.; Siao, C.-J.; Berno, A.; Young, P.; Sapolsky, R.; Ghandour, G.; Perkins, N.; Winchester, E.; Spencer, J.; Kruglyak, L.; Stein, L.; Hsie, L.; Topaloglou, T.; Hubbell, E.; Robinson, E.; Mittmann, M.; Morris, M. S.; Shen, N.; Kilburn, D.; Rioux, J.; Nusbaum, C.; Rozen, S.; Hudson, T. J.; Lipshutz, R.; Chee, M.; Lander, E. S. *Science* **1998**, *280*, 1077.

b. Hacia, J. G. *Nature Genetics Suppl.* **1999**, *21*, 42.

c. Ihara, T.; Chikaura, Y.; Tanaka, S.; Jyo, A. *Chem. Commun.* **2002**, 2152.

d. Frutos, A. G.; Pal, S.; Quesada, M.; Lahiri, J. *J. Am. Chem. Soc.* **2002**, *124*, 2396.

e. Kukita, Y.; Higasa, K.; Baba, S.; Nakamura, M.; Manago, S.; Suzuki, A.; Tahira, T.; Hayashi, K. *Electrophoresis* **2002**, *23*, 2259.

f. Brazill, S. A.; Kuhr, W. G. *Anal. Chem.* **2002**, *74*, 3421.

g. Yamashita, K.; Takagi, M.; Kondo, H., Takenaka, S. *Anal. Biochem.* **2002**, *306*, 188.

2) a. Whitcombe, D.; Theaker, J.; Guy, S. P.; Brown, T.; Little, S. *Nat. Biotechnol.* **1999**, *17*, 804.

b. Thelwell, N. Millington, S.; Solinas, A.; Booth, J. A.; Brown, T. *Nucleic Acids Res.* **2000**, *28*, 3752.

3) a. Holland, P. M.; Abramson, R. D.; Watson, R.; Gelfand, D. H. *Proc. Natl. Acad. Sci. U.S.A.* **1991**, *88*, 7276.

b. Woo, T. H. S.; Patel, B. K. C.; Smythe, L. D.; Norris, M. A.; Symonds, M. L.; Dohnt, M. F. *Anal. Biochem.* **1998**, *256*, 132-134.

4) a. Tyagi, S.; Kramer, F. R. *Nat. Biotechnol.* **1996**, *14*, 303.

b. Tyagi, S.; Bratu, D. P.; Kramer, F. R. *Nat. Biotechnol.* **1998**, *16*, 49.

c. Kostrikis, L. G.; Tyagi, S.; Mhlanga, M. M.; Ho, D. D.; Kramer, F. R. *Science* **1998**, *279*, 1228.

5) a. Jenkins, Y.; Barton, J. K. *J. Am. Chem. Soc.* **1992**, *114*, 8736.

b. Rajir, S. B.; Robles, J.; Wiederholt, K.; Kiumelis, R. G.; McLaughlin, L. W. *J. Org. Chem.* **1997**, *62*, 523.

6) Ranasinghe, R. T.; Brown, L. J.; Brown, T. *Chem. Commun.* **2001**, 1480.

7) Sando, S.; Kool, E. T. *J. Am. Chem. Soc.* **2001**, *124*, 2096.

8) For nonsequence specific fluorescent dyes, such as ethidium, thiazole orange and oxozole yellow dimers, see:

a. Rye, H. S.; Yue, S.; Wemmer, D. E.; Quesada, M. A.; Haughland, R. P.; Mathies, R. A.; Glazer, A. N. *Nucleic Acids Res.* **1992**, *20*, 2803.

b. Cosa, G.; Focsaneanu, K. S.; McLean, J. R. N.; McNamee, J. P.; Scaiano, J. C. *Photochem. Photobiol.* **2001**, *73*, 585.

9) a. Seifert, J. L.; Connor, R. E.; Kushon, S. A.; Wang, M.; Armitage, B. A. *J. Am. Chem. Soc.* **1999**, *121*, 2987.

b. Wang, M.; Silva, G. L.; Armitage, B. A. *J. Am. Chem. Soc.* **2000**, *122*, 9977.

10) For distamycin-Hoechst hybrids, see:

a. Satz, A. L.; Bruice, T. C. *Bioorg. Med. Chem.* **2000**, *8* (*8*), 1871.

b. Satz, A. L.; Bruice, T. C. *J. Am. Chem. Soc.* **2001**, *123* (*11*), 2469.

c. Satz, A. L.; Bruice, T. C. *Bioorg. Med. Chem.* **2002**, *10*, 241.

11) Dervan, P. B. *Bioorg. Med. Chem.* **2001**, *9*, 2215-2235.

12) a. Janssen, S.; Durussel, T.; Laemmli, U. K. *Mol. Cell* **2000**, *6* (5), 999.

b. Maeshima, K.; Janssen, S., Laemmli, U. K. *EMBO J.* **2001**, *20*, 3218.

13) Gygi, M. P.; Ferguson, M. D.; Mefford, H. C.; Kevin, P. L.; O'Day, C.; Zhou, P.; Friedman, C.; van den Engh, G.; Stobwitz, M. L.; Trask, B. J. *Nucleic Acids Res.* **2002**, *30*, 2790.

14) Kubin, R. F.; Fletcher, A. N. *J. Luminescence* **1982**, *27*, 455.

15) Trauger, J. W.; Dervan, P. B. *Methods Enzymol.* **2001**, *340*, 450.

16) a. Lakowicz, J. R. *Principles of Fluorescence Spectroscopy*; Plenum Press: New York, 1983.

b. Johansson, M. K.; Fidder, H.; Dick, D.; Cook, R. M. *J. Am. Chem. Soc.* **2002**, *124*, 6950.

c. Rabinowitch, E.; Epstein, L. F. *J. Am. Chem. Soc.* **1941**, *63*, 69.

17) Addition of a four-ring polyamide to TMR (intermolecular association) affords a 10 nm bathochromic absorption maximum shift of TMR, similar to that observed for conjugates **1**-**6** (vs control TMR **7**). Fluorescence emission data in the presence of linearly increasing polyamide concentration affords a linear Stern-Volmer plot.[16]

18) Although polyamide-Hoechst hybrids[10] have the property of enhanced fluorescence when bound to match DNA, the minor groove binding Hoechst dye requires an A/T tract adjacent to the DNA target site and hence is not as versatile.

19) White, S.; Baird, E. E.; Dervan, P. B. *Chem. Biol.* **1997**, *4*, 569.

20) Yang, X.-L.; Hubbard IV, R. B.; Lee, M.; Tao, Z.-F.; Sugiyama, H.; Wang, A. H.-J. *Nucleic Acids Res.* **1999**, *27*, 4183.

21) Baird, E. E.; Dervan, P. B. *J. Am. Chem. Soc.* **1996**, *118* (26), 6141.

Chapter 3B

Progress towards Applications Using Fluorophore-Polyamide Conjugates in Genomic Analysis

Background and Significance

The completion of the human genome sequencing initiative is possibly the most remarkable accomplishment in the life sciences since Watson and Crick first described the DNA double helix. However, the vast potential of this new resource in the field of human medicine demands that the three-dimensional significance of its linear sequence be understood in greater detail. Beyond the scope of diseases with genetic origins, the tools of genomic analysis are also well suited to combating the growing threat posed by pathogenic bacteria and viruses.

The array of technologies developed for large-scale genome sequencing relies heavily on fluorescent oligonucleotide probes for specific detection of DNA, and though efficient in sequencing applications, these probes are less suited to DNA detection in more physiologically relevant contexts and require sample denaturation for effective function. The needs of genomic analysis in the "post-genome" era might be at least partially addressed by using fluorophore-polyamide conjugates for DNA detection. These ligands can target a wide range of predetermined DNA sequences, in both condensed states and in protein-complexes (Figure 3.7).[1,2] Further advantages are proffered by the versatility and efficiency of polyamide synthesis as well as by the discovery of conjugates that exhibit pronounced fluorescent enhancement upon binding their target DNA sequences.

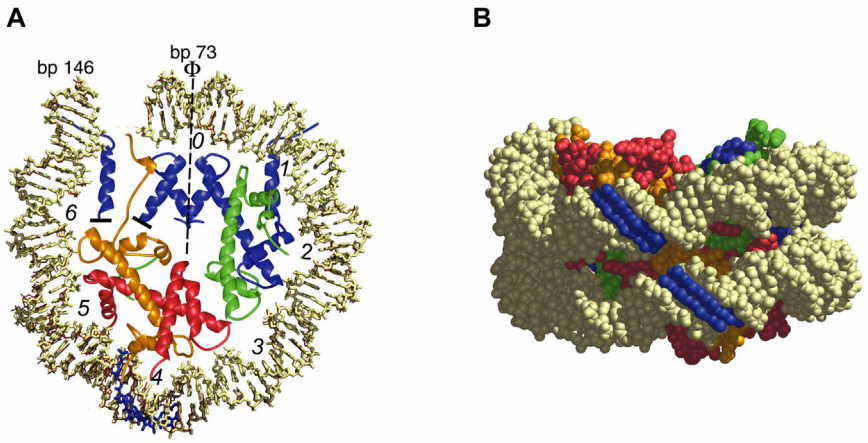

Figure 3.7 X-ray co-crystal structure of nucleosome core particle-polyamide complex (PDB code 1M18)[2]. **(A)** Structure viewed down the superhelical axis. Associated proteins (H3, blue; H4, green; H2A, yellow; H2B, red) and superhelix locations are shown. Associated polyamides are shown in blue. **(B)** Side view of the NCP-polyamide complex.

Fluorophore-polyamide conjugates have already found use in chromosome staining as recognition elements for telomeric and centromeric repeat sequences. Given the biological importance of repetitive DNA satellite sequences and their frequent incompatibility with hybridization-based techniques, polyamides may provide a powerful alternative for repeat detection. Of course, polyamide-based detection can also be extended to other sequences, providing a non-destructive alternative to restriction enzymes for detection in optical mapping.

Tetramethylrhodamine-Polyamide Conjugates as Probes for dsDNA

The DNA recognition properties of the compounds described in Chapter 3A, as determined by DNase I footprinting on designed plasmids (Figure 3.8), validate their promise as sequence specific probes for dsDNA. These findings, as well as the observed quenching phenomenon, were unexpected in light of previous work with fluorophore-polyamide conjugates. Specifically, hairpin polyamides bearing

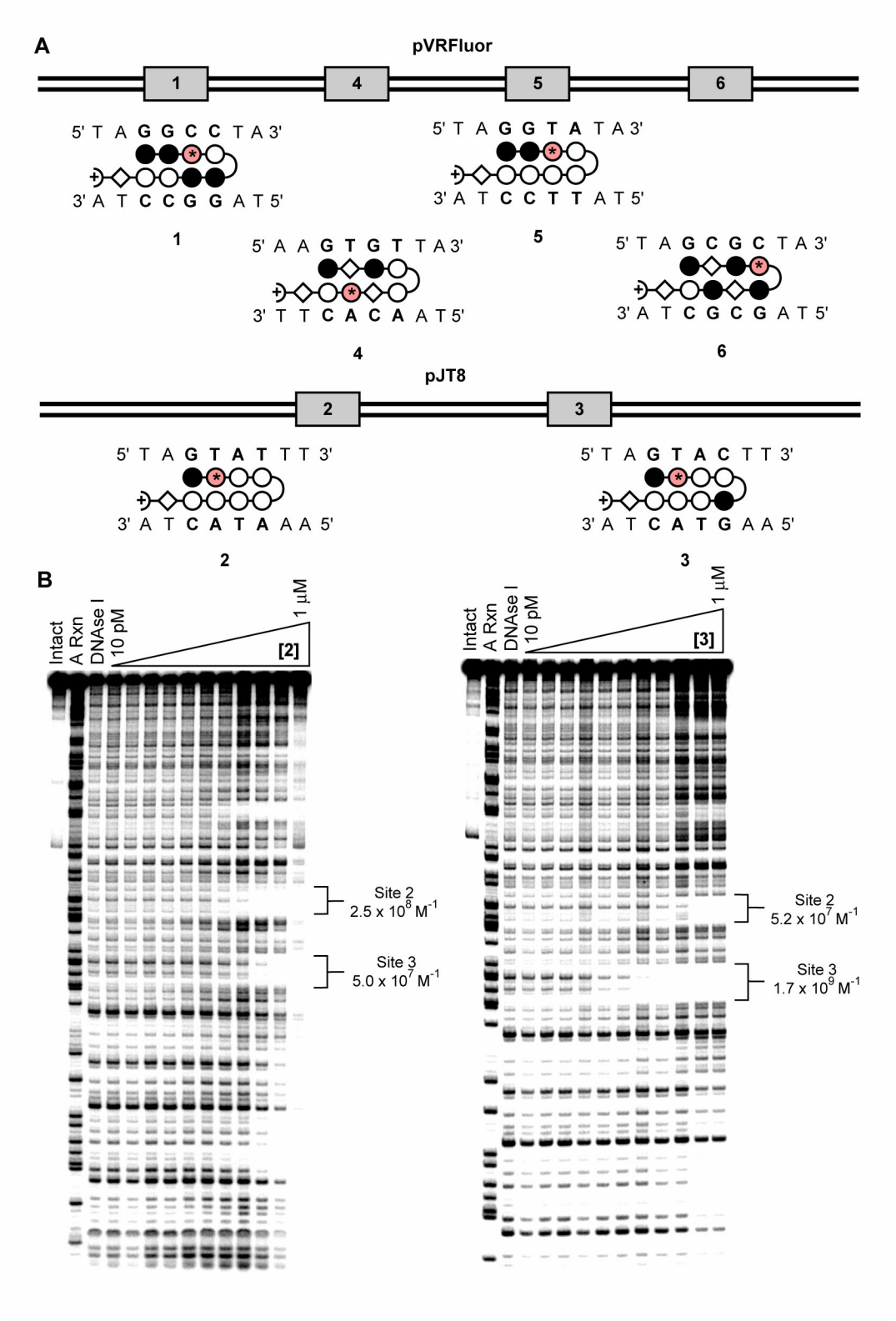

Figure 3.8 DNA recognition properties of TMR-hairpin polyamide conjugates. (A) Two designed plasmids were designed to contain match binding sites for conjugates 1-6. (B) Quantitative DNase I footprinting titration were used to determine the association constants of conjugates 1-6 at each binding site (representative gels for 1 and 2 are shown).

related or distinct fluorescent probes, with different chemical linkers and sites of polyamide attachment (Figure 3.9), had previously been shown to possess diminished affinities and specificities for their cognate DNA sequences (Table 3.3). Subsequent re-examination of their fluorescence properties revealed little or no fluorescent enhancement upon association with DNA, suggesting that the conjugates described in Chapter 3A are in some way unique in the realm of fluorophore-polyamide conjugates.

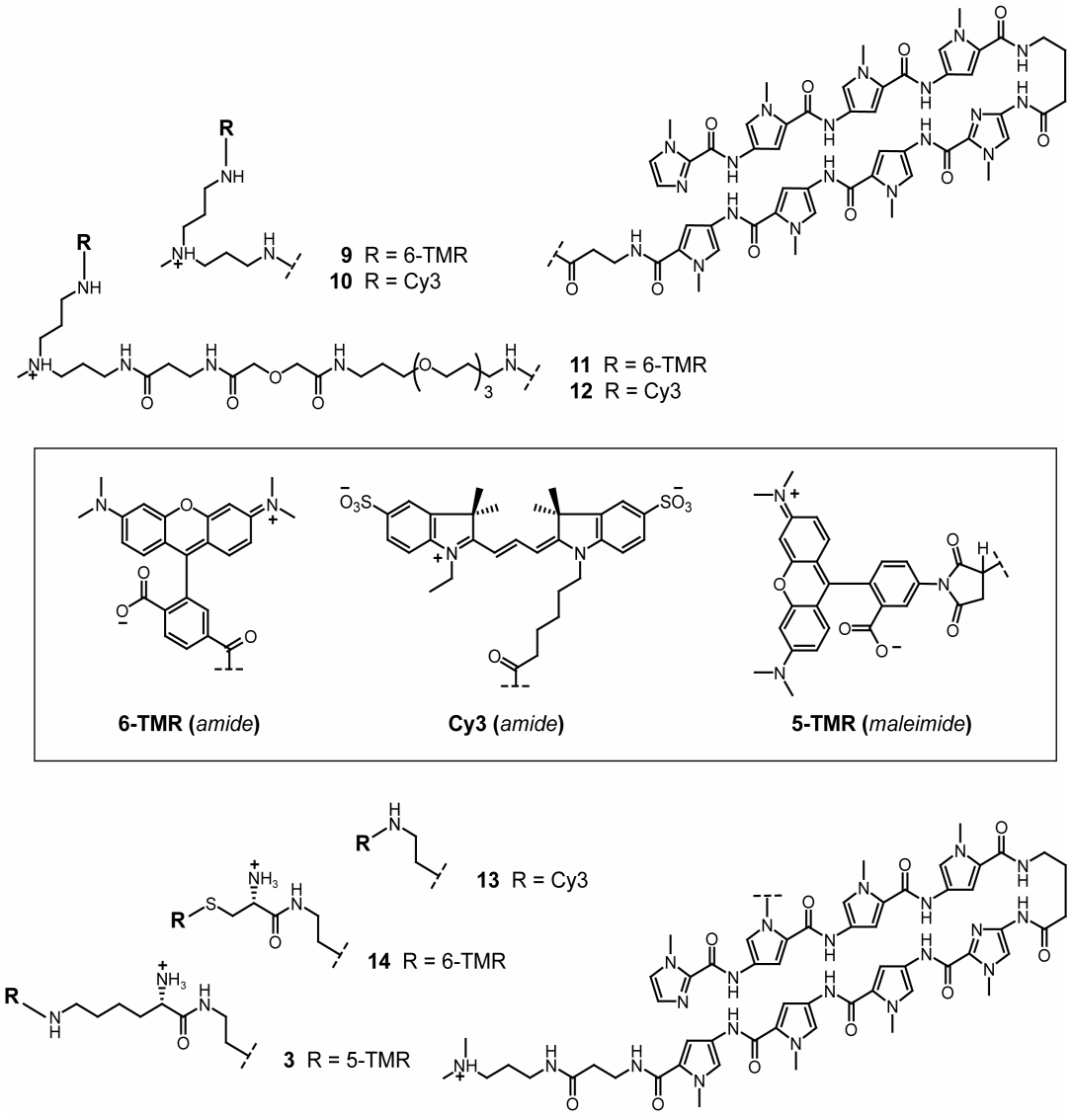

Figure 3.9 Chemical structures of different classes of fluorophore-polyamide conjugates.

Table 3.3 Physical properties of different classes of fluorophore-polyamide conjugates.

Polyamide Conjugate	Fluorophore R	λ_{max}	K_A (5' TAGTACTA 3') match site	Fluroescent Enhancement
3	5-TMR (maleimide)	550 nm	1.7×10^9 M^{-1}	++
9	6-TMR (amide)	548 nm	1.0×10^7 M^{-1}	-
10	Cy3 (amide)	554 nm	5.7×10^7 M^{-1}	-
11	6-TMR (amide)	548 nm	2.0×10^7 M^{-1}	-
12	Cy3 (amide)	554 nm	6.4×10^7 M^{-1}	-
13	Cy3 (amide)	557 nm	1.0×10^9 M^{-1}	+
14	6-TMR (amide)	548 nm	5.0×10^7 M^{-1}	-

Centromere Staining in Cytogenetic Chromosome Spreads

The first applications of fluorescently-labeled polyamide conjugates in detection of satellite DNA sequences were reported by Laemmli and co-workers.[3,4] Both 1:1 and hairpin motifs, bearing C-terminal fluorescein or Texas Red probes, were used to stain 5'-GAGAA-3' repeats in *Drosophila* as well as telomeric repeats in insects and humans (5'-TTAGG-3' and 5'-TTAGGG3', respectively). Trask and colleagues have described similar experiments, using hairpin conjugates to stain centromere repeats (5'-TTCCA-3') on human chromosomes, both in cytogenetic spreads and in conjunction with flow cytometry.[5]

In combination, telomere- and centromere-specific stains might allow the dynamics of chromosome structure to be examined in the context of living cells. Such an application requires, *a priori*, that the selected polyamide stains be localized in the nucleus, and while polyamide research in this field is ongoing, design principles that allow nuclear uptake are becoming more evident. The first generation of centromere-targeted polyamides (Figure 3.10A), employed by the Trask group, though effective in cytogenetic preparations, is not optimal for the *in vivo* application

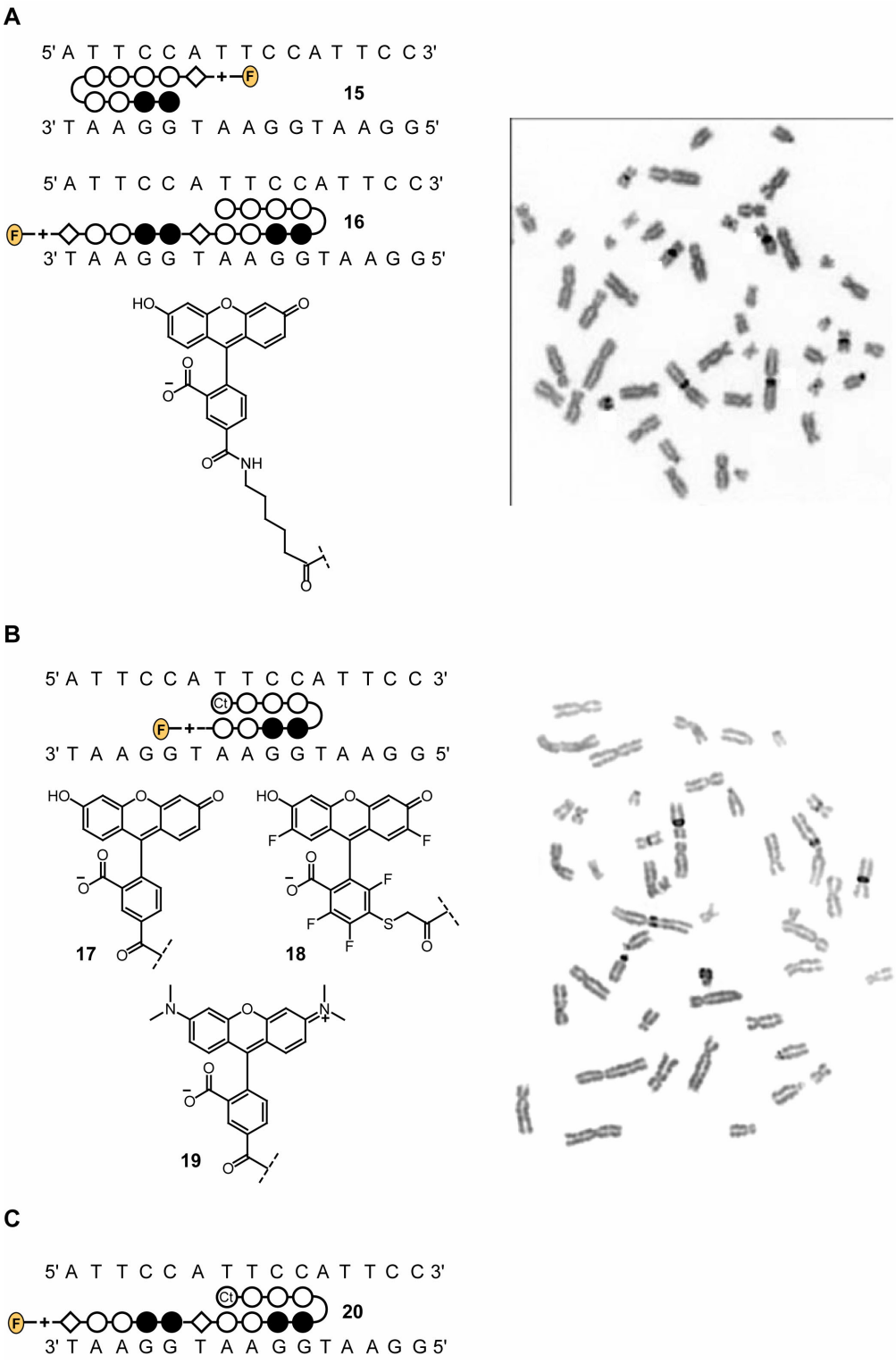

Figure 3.10 Application of fluorophore-polyamide conjugates as centromere-specific chromosome stains. **(A)** First generation centromere-specific polyamide stains (*left*) used by Trask and co-workers in cytogenetic preparations (*right*). **(B)** Second generation polyamide conjugates designed for centromere staining (*left*) were assayed by Trask group in cytogenetic chromosome spreads (*right*). **(C)** Future polyamide design for centromere recognition.

described above. The smaller eight-ring polyamide **15** is advantageous from the standpoint of cell permeability, but is inherently less specific than twelve-ring compound **16**.

A second generation of centromere-specific hairpin polyamide conjugates was designed by incorporating a novel T-specific, N-terminal chlorothiophene (Ct) residue (Chapter 5A) to an eight-ring scaffold. Two fluorescein derivatives and a tetramethylrhodamine fluorophore were attached to the C-terminus of the new polyamide scaffold, affording **17**, **18**, and **19**, respectively (Figure 3.10B). In collaboration with the Trask group, these compounds proved capable of chromosome staining in fixed spreads; however, their specificity was still reduced relative the longer twelve ring conjugate **16**. This result is not surprising given that the longer polyamide contains four highly specific Im residues while **17**-**19** are composed of two Im/Py pairings and a moderately selective Ct/Py pairing. The new eight-ring polyamides, including the TMR conjugate, did show nuclear localization in a range of cell lines (Chapter 5B).

The uptake properties of **19** may indicate that the chlorinated cap residue assists nuclear localization, opening the door for two-color experiments with a fluorescein-labeled polyamide conjugate targeting telomere repeats. The specificity of compounds **17**-**19** will be addressed in future generations of centromere stains, using the N-terminal Ct residue within the context of a longer polyamide (Figure 3.10C).

Microsatellite Detection with Fluorophore-Polyamide Conjugates

Satellites are extragenic genomic regions composed of tandemly repeated, usually uninterrupted DNA subsequences.[6] Minisatellites, exemplified by telomeric repeats, typically form clusters up to 25 kb in length with repeat units up to 25 bp. Microsatellites, on the other hand, are composed of 2-6 bp subsequences repeated 10-20 times.[7] Repetitive sequences account for approximately 15% of the human genome, and while their biological relevance is not yet fully understood, their influence on DNA structure in both relaxed and condensed states is thought to affect the accessibility of the double helix to proteins.[8]

The polymorphic nature and widespread occurrence of microsatellites, in all organisms tested to date, have made them particularly attractive markers for forensic identification and DNA profiling.[9] Trinucleotide repeats have also been linked to several neurodegenerative disorders including Huntington's disease (Table 3.4).[10] A majority of the repeat sequences thus far linked to disease states can be targeted with hairpin polyamides; however, purine repeats are often characterized by structural variations that preclude hairpin binding. These sequences can be recognized with the 1:1 polyamide motif, often with affinities and specificities that rival those of the hairpin motif.[11]

Table 3.4 Trinucleotide repeat sequences associated with human diseases.[7-10]

Disease	Repeat	Normal Frequency	Disease Frequency	Location	Biological Effect
Fragile XA	5' CGG 3'	6-52	> 200	5' untranslated region	promoter methylation; gene silencing
Fragile XF		7-40	> 300	?	
Jacobsen Syndrome		11	80	?	
Fragile XE	5' GCC 3'	6-25	200-900	?	?
Myotonic Dystrophy	5' CTG 3'	5-37	80-1000	3' untranslated region	altered chromatin structures
Huntington's Disease	5' CAG 3'	10-34	40-121	coding region	Polyglutamine expansion
Kennedy Syndrome		11-34	40-55	coding region	
Spinocerebellar ataxia 1-7		6-30	> 30	coding region	
Friedreich's ataxia	5' GAA 3'	6-29	200-900	intron	altered transcription

The ability of 1:1 polyamides to recognize purine repeats was examined on a designed plasmid by quantitative DNase I footprinting (Figure 3.11A). Three distinct purine repeats, 5'-GAA-3', 5'-GAAA-3', and 5'-GGA-3', as well as a control site, were screened for binding of polyamides **21**-**23** (Figure 3.11B). The results show that the 1:1 motif can be used to bind two of the above sequences with good affinity and specificity (Figure 3.12). None of the polyamides tested showed appreciable (> 10^7 M^{-1}) binding to the 5'-GGA-3' site, however, the other two repeat sites were bound by designed polyamides. The affinity of **21** and **23** for these sites is lower than might be desired; however, their specificity for a repeated sequence should offset the impact of lower association constants on signal-to-noise ratios. The 1:1 motif can also be extended to longer binding sites with less severe contributions to molecular weight relative to hairpin polyamides.

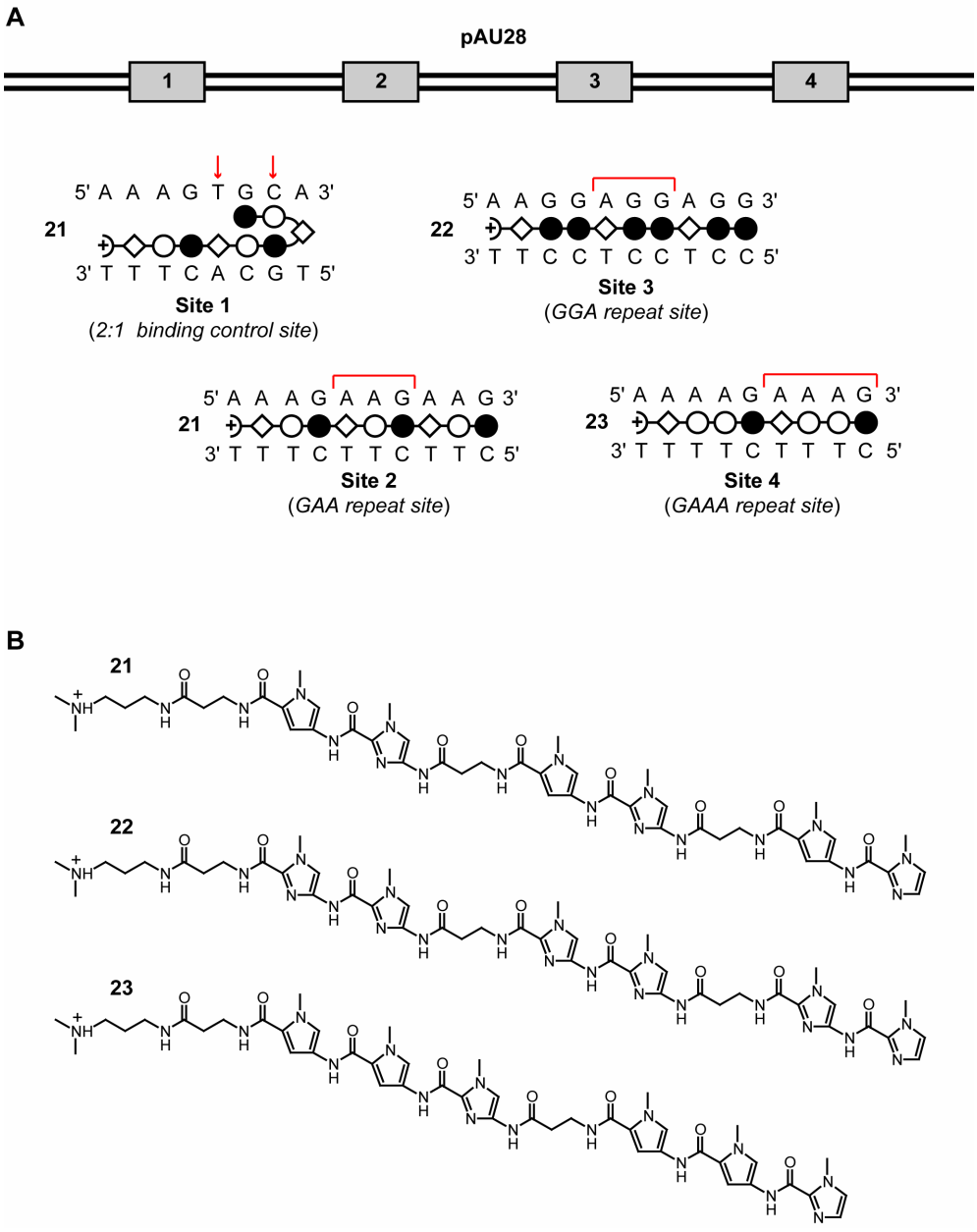

Figure 3.11 Designed plasmid and polyamides for recognition of purine repeat sequences with the 1:1 motif. **(A)** A plasmid containing three purine repeat sites as well as a control site was used to screen the DNA-binding properties of polyamides **21**-**23**. Red arrows represent pyrimidine interruption of purine tract and red lines show repeat unit of purine tract. **(B)** Chemical structures of designed 1:1 polyamides **21**-**23**.

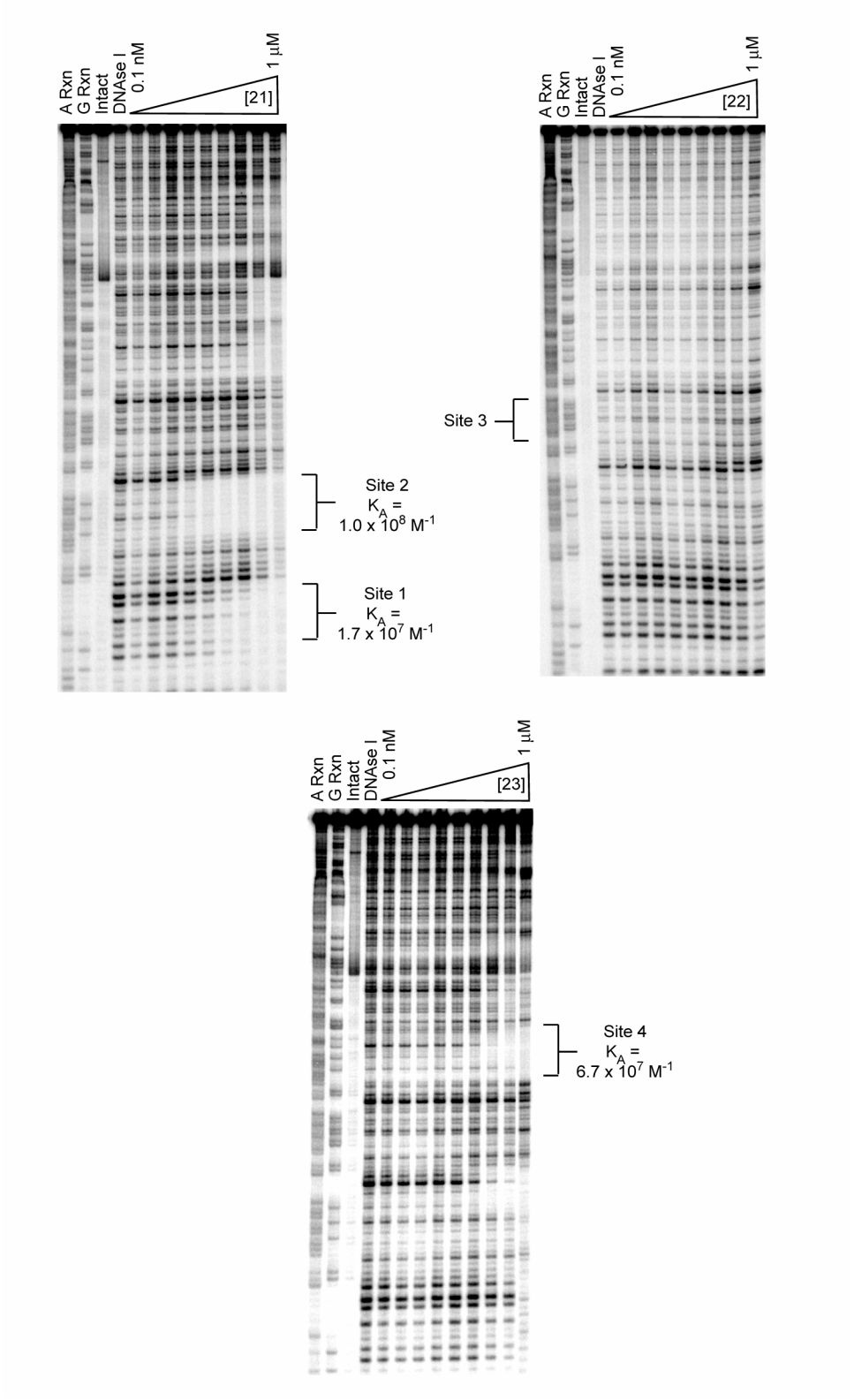

Figure 3.12 Quantitative DNase I footprinting gels for compounds **21**-**23** performed on plasmid pAU28. Gels include A and G sequencing reactions, intact and digested control lanes, with no polyamide, and polyamide concentrations from 0.1 nM to 1 μM.

Physical Genome Mapping with Polyamide Conjugates

The viability of fluorophore-polyamide conjugates for sequence specific detection of both short DNA sequences, as well as repeated sequences in chromosomal contexts, demonstrates a fraction of their potential in genomic analysis. However, a substantial set of physical techniques, including restriction fingerprinting and optical mapping, are applicable on intermediate scales between the above extremes, and while these methods were once used primarily to refine and direct genome sequencing efforts, their utility in the "post-genome" era should not be overlooked. Aside from their use in sequencing resistant bacterial strains and pathogenic viruses, both methods provide the means to determine physical distances between genetic markers, allowing the organizational and regulatory features of genomes to be addressed in molecular detail. Thus, detailed physical maps are immediately relevant to understanding the genetic origins of complex, polygenic human disease states and may offer insight to novel therapeutic strategies.

The classical mapping technique, illustrated in Figure 3.13A, uses restriction enzymes in conjunction with gel electrophoresis to assess genetic diversity evidenced by restriction fragment length polymorphisms (RFLP).[12] The sequence contexts of the separated fragments are then determined by Southern blot hybridization with labeled oligonucleotide probes. This technique is labor-intensive and requires large amounts of DNA; however, these limitations can be partially circumvented by PCR with primers designed to flank the genomic region of interest. While several distinct DNA mutations can be identified by RFLP analysis, its most

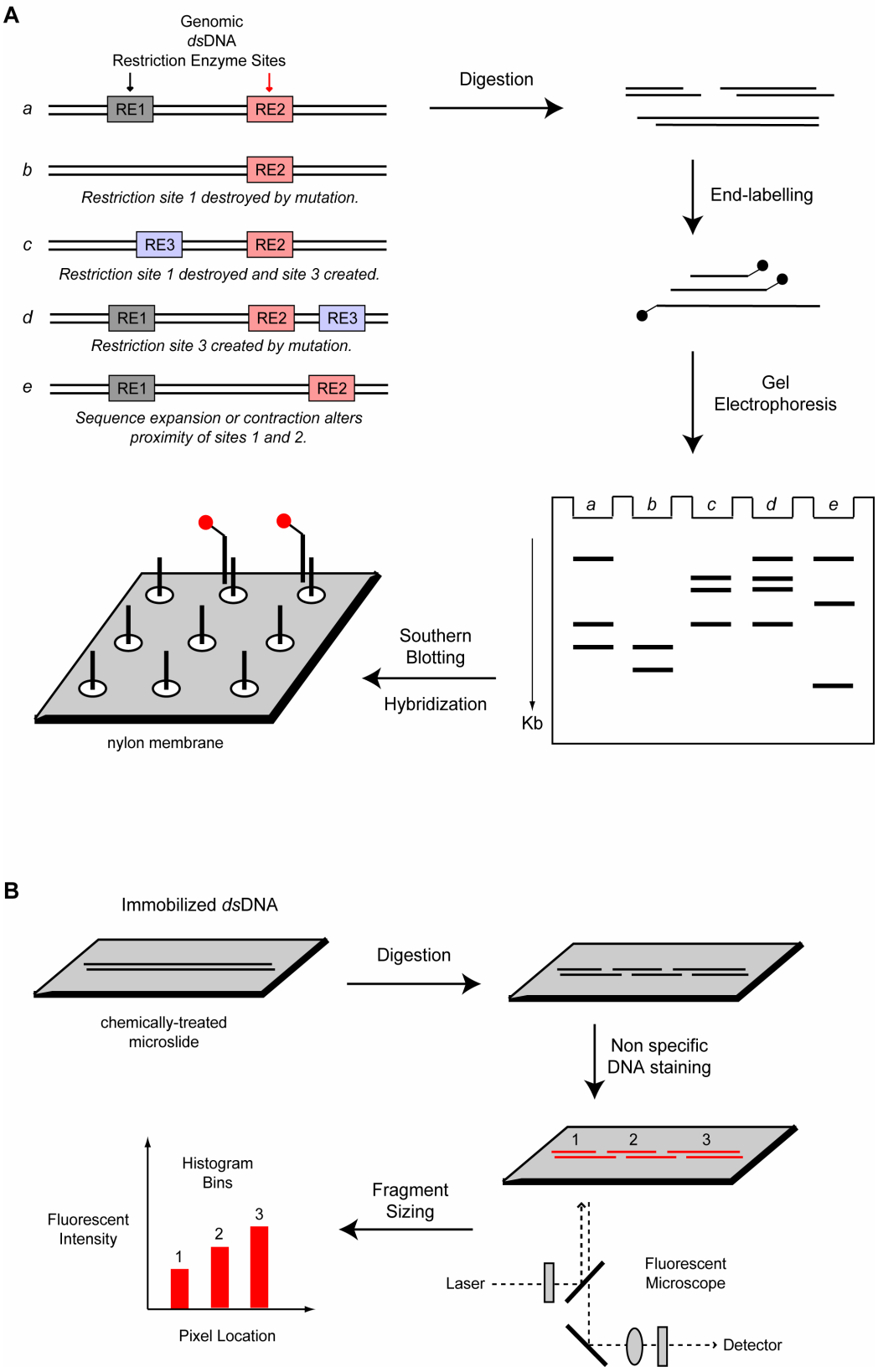

Figure 3.13 Physical methods of genome mapping. **(A)** Classical RFLP-based technique for genomic analysis using restriction enzymes in conjunction with gel electrophoresis and Southern blotting. **(B)** Optical mapping strategy using restriction enzymes and fluorescent DNA stains for single molecule analysis of DNA molecules.

powerful application examines hypervariable regions (HVR) containing tandem arrays of repeated DNA sequences. This application, first developed in 1985, still forms the basis of forensic identification and paternal assessment today.[13]

Despite refinements in RFLP analysis over the last three decades, it is still limited by a dependence on electrophoresis to separate digested fragments, as well as the necessity of prior sequence knowledge of the genomic area of interest. The development of multiplex capillary electrophoretic methods and microfluidic devices for DNA separation has addressed the former limitation of RFLP,[14] although informative genetic markers are often repetitive in nature and cannot be always be resolved by standard techniques. The necessity of prior sequence knowledge for design of oligonucleotide probes or PCR primers is inherent to the technique and cannot be circumvented.

An alternative technique for obtaining high-resolution physical maps has been developed using single molecule spectroscopy. Optical mapping uses chemically-derivatized surfaces for immobilization of DNA which is subsequently digested with restriction enzymes (Figure 3.13B).[15,16] The digested sample is then stained with non-specific, fluorescent probes and restriction sites are visualized as gaps in single DNA molecules. The DNA-binding stoichiometry of the fluorescent probe can then be used to calculate the size of restriction fragments based upon their fluorescent intensity. Similar protocols could potentially be employed using microfluidic devices, allowing simultaneous sizing and sorting.

Both classical RFLP and modern optical methods of genome mapping rely heavily on fluorescent DNA probes. Oligonucleotide probes require sample

denaturation before hybridization, greater care in handling, and more labor input for synthesis, relative to polyamide conjugates. An assortment of commercial DNA stains, with different absorption-emission profiles, are available and protocols for their use have been optimized. These proprietary compounds show dramatic fluorescent enhancement upon bis-intercalation of dsDNA, providing high signal-to-noise (S/N) ratios in bulk solution as well at the single molecule level.[17-19] Non-specific intercalation at regular intervals all across the double helix often limits the compatibility of these stains with other DNA-binding molecules or with condensed DNA states. The specificity and non-invasive nature of minor groove-binding polyamides are thus desirable at least in the context of two color experiments.

Polyamides as Sequence Specific DNA Stains

S/N ratios become increasingly important when moving from short sequences to larger genomic contexts. The effective concentration range of the probe, its detection limit, and its compatibility with a range of buffers are all factors that contribute to the overall utility of the stain both in bulk solution and on the single molecule level. The above features of a series of fluorophore-hairpin polyamide conjugates (Figure 3.14) were investigated in bulk solution using lambda DNA as a model system. This model has been studied extensively by single molecule techniques, and its size (48 Kb) is relevant to physical mapping techniques.

The performance of hairpin conjugates in genomic contexts is strongly influenced by their inherent specificities as well as by the uniqueness of their target sites in the DNA fragment of interest. The degeneracy of Py/Py pairings for T, A

relegates Im/Py pairings as the only specific elements in the hairpins studied. Greater Im/Py content therefore enhances the specificity of a given polyamide, enhancing its S/N ratio in the presence of excess mismatch binding sites. The structural content of a hairpin polyamide also affects its S/N ratio by altering the degree of fluorescence quenching that occurs in the absence of DNA. In this regard, aliphatic β residues are less efficacious than Py or Im. The specificity and structural content of the hairpins investigated, as well as the occurrence of their match sites in lambda DNA are summarized in Table 3.5. Titrations of fluorophore conjugates with lambda DNA, monitored by fluorescent detection in microplates as described in Chapter 3A, were used to assess the potential of polyamides as DNA stains.

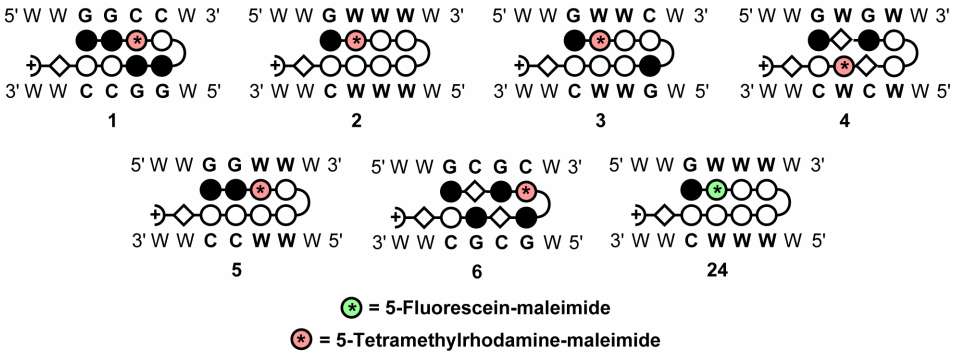

Figure 3.14 Ball-and-stick representations of TMR- and fluorescein-hairpin polyamide conjugates examined in microplate titrations with λ DNA.

Table 3.5 Properties of TMR- and fluorescein-polyamide conjugates examined in microplate titrations with λ DNA.

Conjugate	Specific Pairings	Ring Content	Match Sites (λ DNA)	1 bp Mismatch Sites (λ DNA)
1	4 / 4	8 / 8	128	1334
2	1 / 4	8 / 8	1007	7994
3	2 / 4	8 / 8	386	4560
4	2 / 4	6 / 8	302	4102
5	2 / 4	8 / 8	427	4488
6	4 / 4	6 / 8	110	1558
24	1 / 4	8 / 8	1007	7994

The linearity of fluorescent intensity and fold-fluorescent enhancement of conjugates **1**-**6** in the presence of increasing concentrations of lambda DNA (λ) is illustrated in Figure 3.15. The commercial DNA stain, SYTOX-orange is included for reference. Detection limits for these conjugates relative to the commercial stain can be inferred from the above data; however, such an interpretation neglects the greater number of binding sites available to the non-specific intercalator.

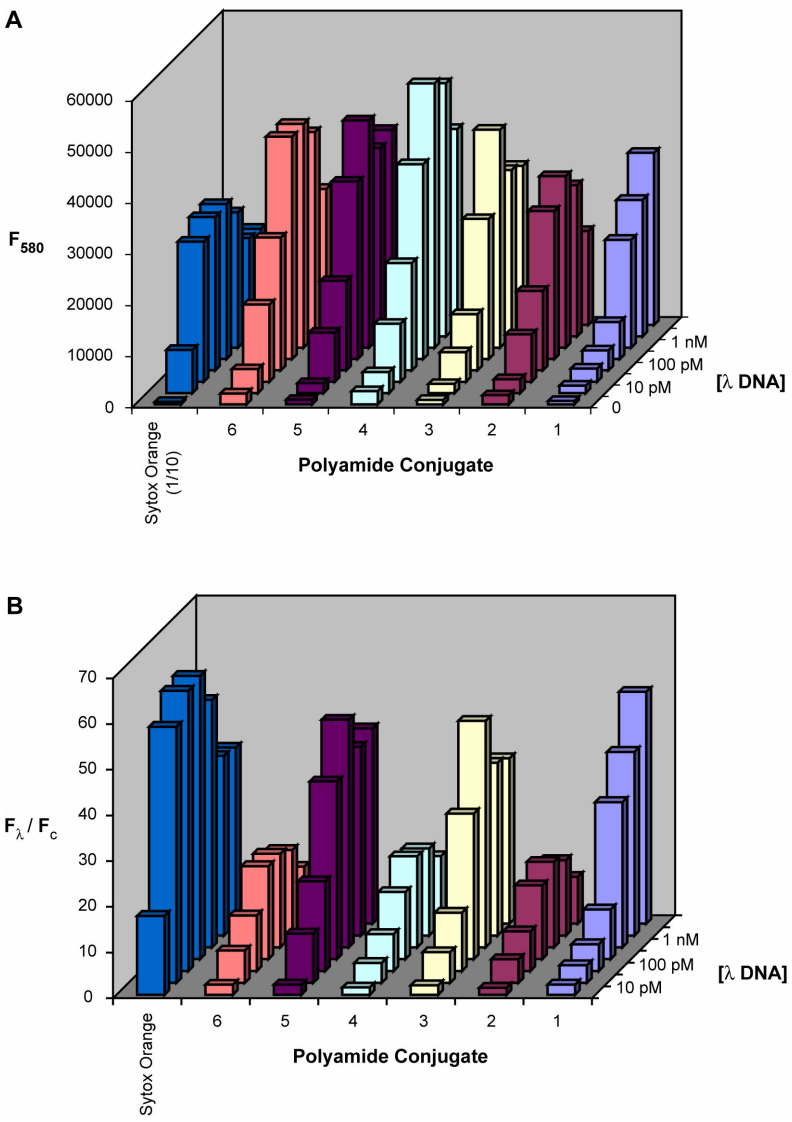

Figure 3.15 Fluorescent response of conjugates 1-6 in the presence of increasing concentrations of λ DNA. **(A)** Fluorescent intensity of conjugates measured at 580 nm plotted as a function of [λ DNA]. Sytox Orange values shown as 10% measured values for purposes of scale. **(B)** Fold fluorescent enhancement determined relative to no DNA control.

Microplate experiments using combinations of TMR-hairpin conjugates in the presence and absence of λ DNA were also performed (Figure 3.16A). Eight-ring conjugates were selected to minimize differences in signal resulting from decreased quenching in the absence of DNA. The selected hairpins, **1**-**3** and **5**, possess inherently different specificities and target site frequencies in λ DNA. Cursory examination of the results would lead one to assume that mixtures of polyamides are not effective for staining, as both signal (with λ DNA) and background (no λ DNA) are diminished relative to values predicted from 1-component experiments (Figure 3.16B). The decreased background level could be a result of intermolecular association in the unbound state which magnifies the quenching phenomenon. The decreased level of signal for 3- and 4-component mixtures in the presence of λ DNA is probably an optical artifact arising from the high concentration of fluorophore conjugates (1.5 μM and 2 μM, respectively). Standard titrations using a single polyamide conjugate at these concentrations also gives reduced signal; however, the reduced fluorescent intensity of 2-component mixtures requires a different explanation.

When considering polyamide behavior in large DNA fragments, the overall accessibility and frequency of match binding sites and single base pair mismatch sites must be considered. Overlapping or adjacent match binding sites may disfavor stoichiometric association of ligand, resulting in artificially decreased signal. These effects are even more relevant to polyamide mixtures as the binding of one ligand could limit the access of a second ligand to a proximal site. The fluorescent intensities of relatively non-specific polyamides, on the other hand, might be

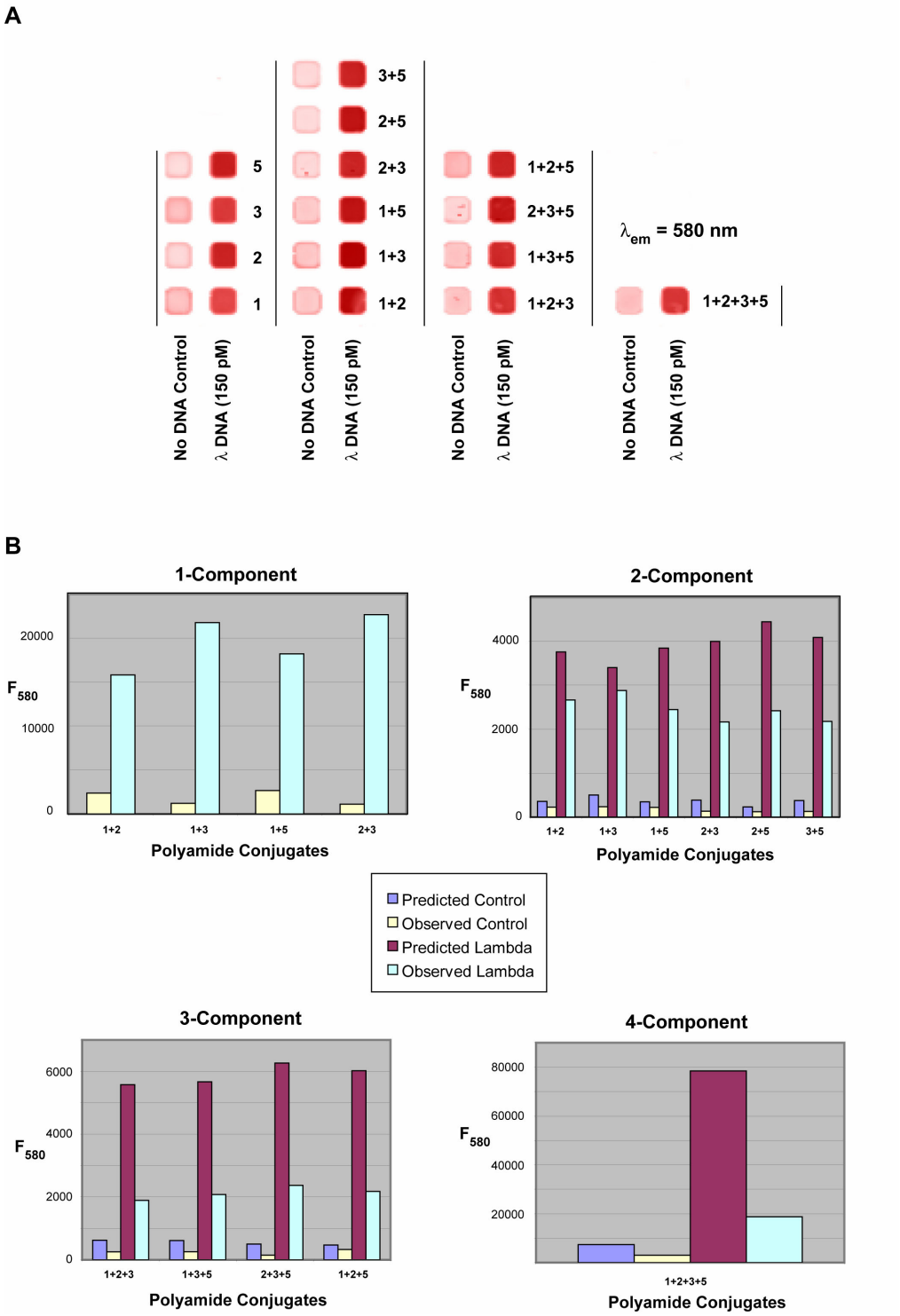

Figure 3.16 One-color synergy experiments using TMR-hairpin polyamide conjugates with λ DNA. **(A)** Microplate experimental layout for synergy titrations. Typhoon imaging system was used to measure emission intensity at 580 nm, following excitation at 532 nm. **(B)** Averaged data set from duplicate analyses of microplates. Predicted values for multi-component mixtures are based on 1-component results.

artificially inflated when examined individually, as a result of undesired binding to mismatch sites; however, this undesired binding would be at least partially alleviated if a subset of the available mismatch binding sites were associated with other polyamide conjugates. The data summarized in Figure 3.16B offers some evidence of this effect as binary combinations of **2**, the least specific compound in the series, with other conjugates results in the largest deviation from predicted intensities. In particular, this deviation is most significant for mixtures of **2** with conjugates **3** or **5**, whose target sites are tolerable single base pair mismatches for **2**, as evidenced by DNase I footprinting.

The influence of specificity on staining by polyamide conjugate mixtures was also investigated using a two-color experiment, in which the TMR moiety of **2** was replaced with a fluorescein probe to give **24** (Figure 3.17A). Conjugates of this type are known to show the exhibit the same quenching phenomenon as their rhodamine counterparts, however, the emission of these fluorophores is distinct, allowing the binding of **24** to be reliably measured in the presence of multiple TMR conjugates. The data from two-color titrations supports the inferences made from one-color results (Figure 3.17B). The fluorescent intensity of **24**, measured at 526 nm, is increasingly attenuated by the presence of **1**, **3**, and **5** in line with the deviations observed above. The binding of TMR conjugates is evident based upon their fluorescent intensities, measured at 580 nm.

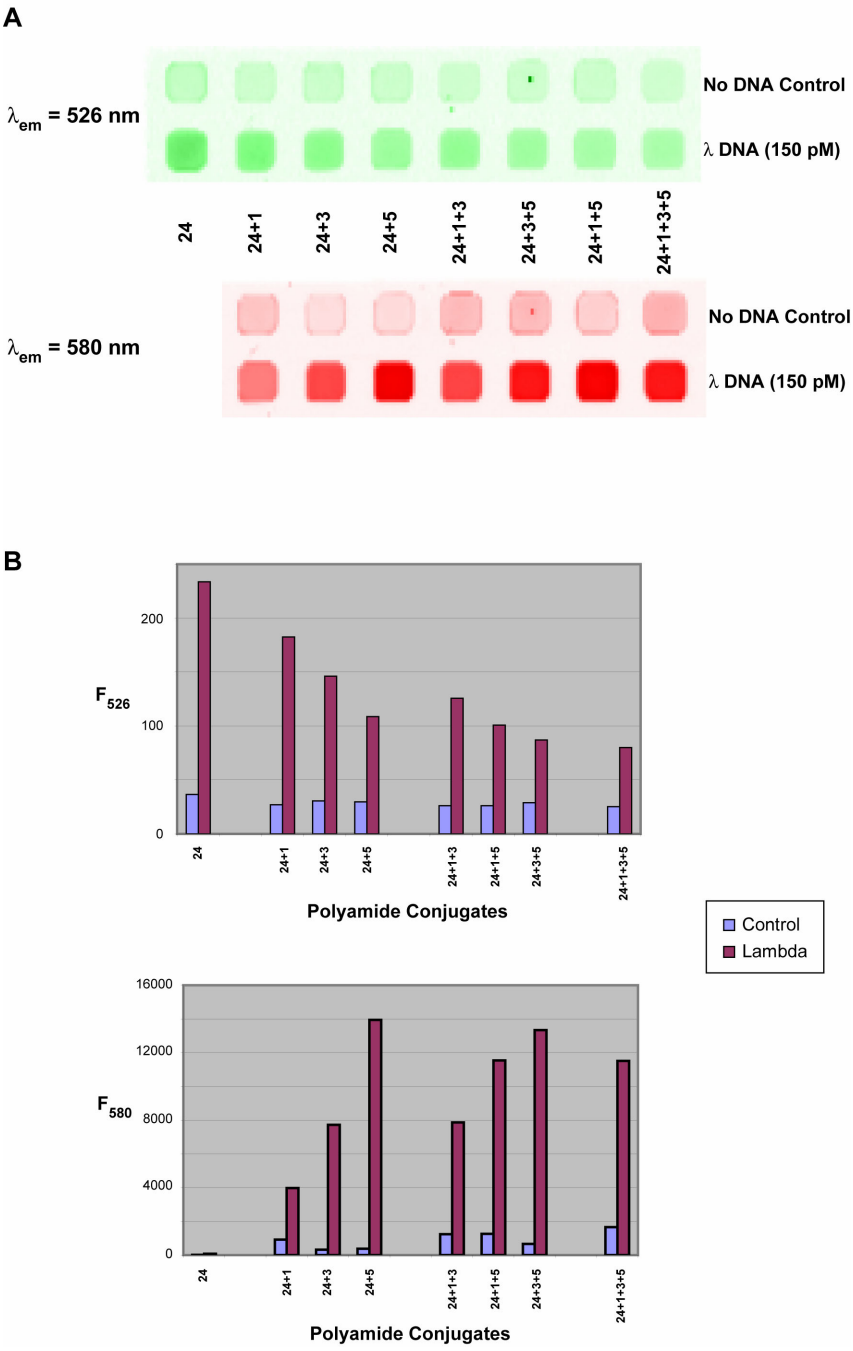

Figure 3.17 Two-color synergy experiments using TMR- and fluorescein-hairpin polyamide conjugates with λ DNA. **(A)** Microplate experimental layout with emission at 526 nm shown in green-scale and emission at 580 nm shown in red-scale. Intensities were measured using Typhoon imaging system with excitation at 532 nm. **(B)** Averaged data set from duplicate microplate experiments.

Different handling conditions and buffers were examined for conjugates **1**-**6** and **24**, in the context of both the model system and smaller hairpin oligonucleotides.

Ambient conditions and short equilibration times (1-2 hours) gave reproducible results with little variation in fluorescent intensity in microplate experiments. Tris-EDTA buffer systems containing various concentrations of monovalent and divalent cations, at pH 7-8, were all effective, though Tris-EDTA with 5 mM NaCl proved slightly better than other buffer systems initially examined. A more detailed investigation was subsequently undertaken to assess the S/N ratio of polyamide conjugate **3** in four different restriction enzyme buffers, with and without added BSA (Figure 3.18A). Concentrated NEBuffers 1-4 were obtained as concentrated stock solutions from New England Biolabs. The 1x compositions of these buffers are as follows: NEBuffer 1 (10 mM Bis Tris Propane·HCl, 10 mM $MgCl_2$, 1 mM DTT, pH 7), NEBuffer 2 (50 mM NaCl, 10 mM Tris·HCl, 10 mM $MgCl_2$, 1 mM DTT, pH 7.9), NEBuffer 3 (100 mM NaCl, 50 mM Tris·HCl, 10 mM $MgCl_2$, 1 mM DTT, pH 7.9), and NEBuffer 4 (50 mM potassium acetate, 20 mM Tris·acetate, 10 mM magnesium acetate, 1 mM DTT, pH 7.9). Addition of BSA to a final concentration of 100 μg/mL was examined for the restriction buffers above as well as a TE control.

The influence of different buffers on fluorescent intensity and S/N for conjugate **3** is illustrated in Figure 3.18B. Clearly, restriction buffers are not optimal for DNA recognition by polyamides, though NEBuffer 1 is at least marginally compatible with conjugates. Perhaps more interesting was the finding that addition of BSA to any of the buffers mentioned above resulted in higher S/N ratios. The data seems to indicate that BSA reduces the fluorescent intensity of fluorophore conjugates both in the presence and absence of DNA.

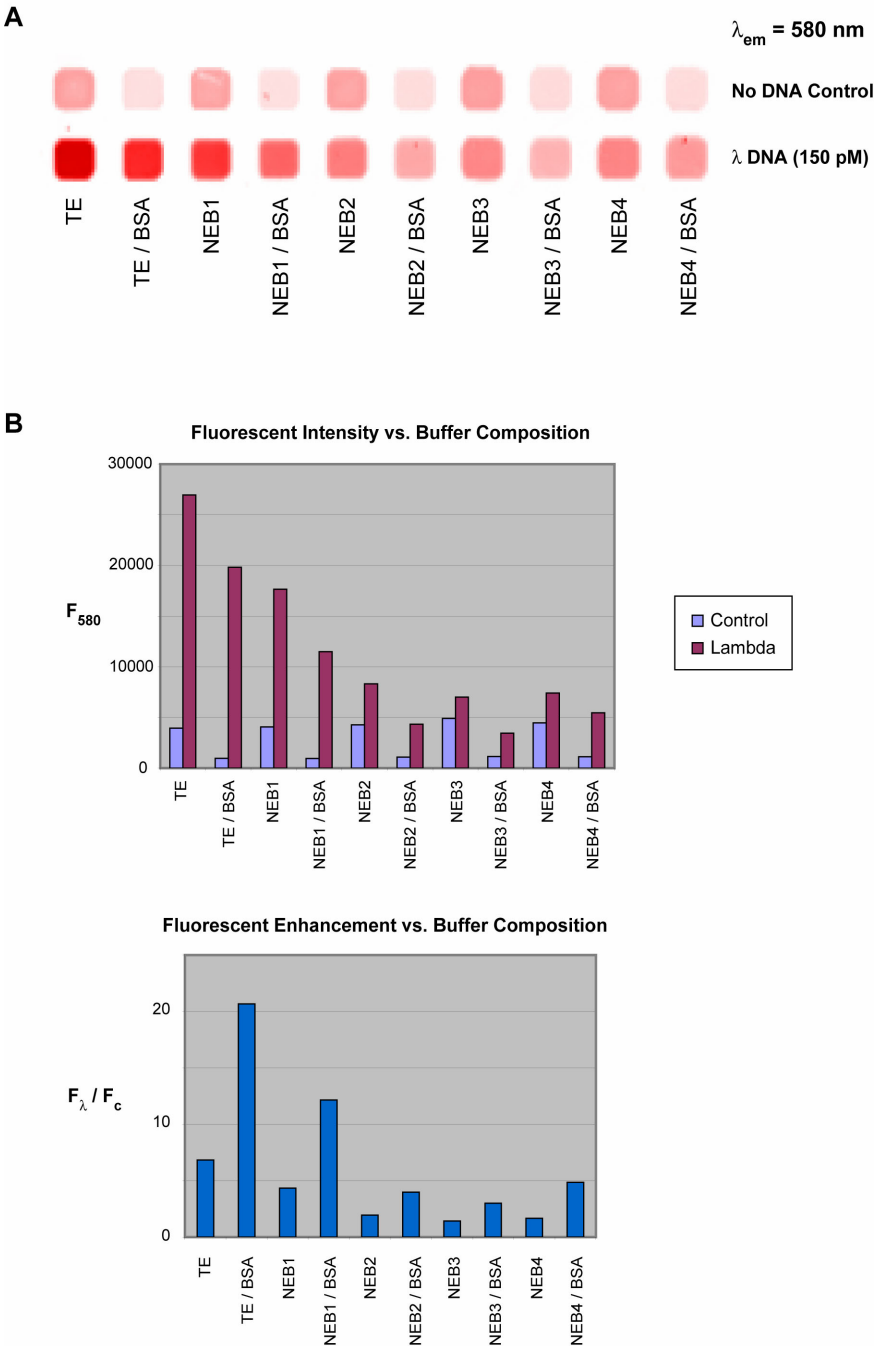

Figure 3.18 Buffer compatibility of TMR-hairpin polyamide conjugates. **(A)** Microplate experimental layout with emission at 580 nm shown in red-scale. Data was collected on Typhoon imaging system with excitation at 532 nm. **(B)** Fluorescent intensity of polyamide conjugates (*top*), in the absence and presence of l DNA, are illustrated for different buffer systems. Fold fluorescent enhancement, relative to a no DNA control, was also determined for different buffer systems.

Future Directions for Quenched Fluorophore-Polyamide Conjugates

Experiments with polyamide conjugates on the single molecule level were conducted in collaboration with the Quake group at Caltech. The goal of these experiments was to visualize fluorophore-hairpin conjugates bound to immobilized λ DNA using a fluorescent microscope. Preliminary work employed polyamide conjugates that must now be considered non-optimal, characterized by poor binding affinities and a lack of fluorescence enhancement in the presence of DNA. Later experiments used the TMR-conjugates described above as well as cyanine-conjugates described in Chapter 4, and while these compounds were more effective than their progenitors, verification of polyamide localization on immobilized DNA proved elusive.

The commercial DNA stains commonly used in optical mapping experiments typically exhibit nanomolar affinities for dsDNA and can influence the overall structure of the double helix and hence the dimensions of the minor groove. These stains were envisioned as means of verifying the association of polyamide conjugates with immobilized DNA; however, their influence on polyamide binding should be evaluated in greater detail before further experiments are conceived. In this regard, immobilization of large DNA fragments on chemically treated surfaces might also influence the structure and accessibility of the minor groove to polyamide conjugates. The interaction of polyamide conjugates with derivatized surfaces should also be considered in future single molecule experiments.

An alternative to the mapping experiments described above could use cocktails of polyamide conjugates to stain immobilized DNA with greater frequency,

obviating the need for a commercial “counterstain.” Polyamide cocktails could be developed using relatively non-specific polyamides for detection at one wavelength and more specific polyamides for detection in a second wavelength. Furthermore, the technical difficulties associated with immobilizing and stretching DNA could be circumvented by examining DNA in more biologically relevant contexts, such as in protein complexes. Polyamides are well suited to this goal, and can also be applied to detection of DNA in microfluidic devices where surface association is not required.

Another potentially powerful application of polyamides in genomic analysis could use fluorescent conjugates in conjunction with restriction enzymes. The resulting stained digests could be examined by flow cytometry, gel electrophoresis, or in single molecule experiments. The most important experimental consideration for these experiments is the accessibility of the target DNA to minor groove-binding polyamides.

References

1) Gottesfeld, J. M.; Melander, C.; Suto, R. K.; Raviol, H.; Luger, K.; Dervan, P. B. *J. Mol. Biol.* **2001**, *309*, 615.

2) Suto, R. K.; Edayathumangalam, R. S.; White, C. L.; Melander, C.; Gottesfeld, J. M.; Dervan, P. B. *J. Mol. Biol.* **2003**, *326*, 371.

3) Janssen, S.; Durussel, T.; Laemmli, U. K. *Mol. Cell* **2000**, *6*, 999.

4) Maeshima, K.; Janssen, S.; Laemmli, U. K. *EMBO J.* **2001**, *20*, 3218.

5) Gygi, M. P.; Ferguson, M. D.; Mefford, H. C.; Kevin, P. L.; O'Day, C.; Zhou, P.; Friedman, C.; van den Engh, G.; Stobwitz, M. L.; Trask, B. J. *Nucleic Acids Res.* **2002**, *30*, 2790.

6) Brown, T. A. *Genomes*; Wiley-Liss: New York, 1999.

7) Goldstein, D. B.; Schlotterer, C. *Microsatellites Evolution and Applications*; Oxford University Press: New York, 1999.

8) Sinden, R. R. *Am. J. Hum. Genet.* **1999**, *64*, 346.

9) Dear, P. H. *Genome Mapping: A Practical Approach*; IRL Press: New York, 1997.

10) Pearson, C. E.; Sinden, R. R. *Curr. Opin. Struct. Biol.* **1998**, *8*, 321.

11) Urbach, A. R. *PhD Thesis*; California Institute of Technology: Pasadena, 2002.

12) Lathrop, G. M.; Lalouel, J. M.; Julier, C.; Ott, J. *Proc. Natl. Acad. Sci. USA* **1984**, *81*, 3443.

13) Jeffreys, A. J.; Wilson, V.; Thein, S. L. *Nature*, **1985**, *314*, 67.

14) Yan, X.; Grace, W. K.; Yoshida, T. M.; Habbersett, R. C.; Velappan, N.; Jett, J. H.; Keller, R. A.; Marrone, B. L. *Anal. Chem.* **1999**, *71*, 5470.

15) Aston, C.; Hiort, C.; Schwartz, D. C. *Methods Enzymol.* **1990**, *303*, 55.

16) Schwartz, D. C.; Samad, A. *Curr. Opin. Biotechnol.* **1997**, *8*, 70.

17) Singer, V. L.; Jones, L. J.; Yue, S. T.; Haugland, R. P. *Anal. Biochem.* **1997**, *249*, 228.

18) Yan, X.; Habbersett, R. C.; Cordek, J. M.; Nolan, J. P.; Yoshida, T. M.; Jett, J. H.; Marrone, B L. *Anal. Biochem.* **2000**, *286*, 138.

19) Gurrieri, S.; Wells, K. S.; Johnson, I. D.; Bustamante, C. *Anal. Biochem.* **1997**, *249*, 44.